Journal of Environmental Management 386 (2025) 125654

Contents lists available at ScienceDirect

Journal of Environmental Management

journal homepage: www.elsevier.com/locate/jenvman

Research article

Vascular macrophytes *versus* charophytes: how the macrophyte type and warming affect the sediment microbial community and the production of greenhouse gases

María A. Rodrigo [a,*], Eric Puche [a], Manuel Muñoz-Colmenares [a], Salvador Sánchez-Carrillo [b]

[a] Cavanilles Institute of Biodiversity and Evolutionary Biology, Universitat de València, Catedrático José Beltrán 2, E-46980, Paterna, València, Spain
[b] Department of Biogeochemistry and Microbial Ecology, Museo Nacional de Ciencias Naturales-CSIC (MNCN-CSIC), Serrano 115 Bis, E-28006, Madrid, Spain

ARTICLE INFO

Keywords:
CH_4-CO_2 emissions
Chara hispida
Myriophyllum spicatum
Plant traits
Sediment microbial composition
Sediment O_2 microprofiles

ABSTRACT

In the global warming context, adaptive management strategies involve the conservation and restoration of inland waters by planning the reintroduction of macrophytes to substantially mitigate greenhouse gas emissions (GHG). The selection of appropriate species is crucial. We studied the influence of two submerged macrophyte species on GHG production, sediment-oxygen microprofiles, and microbial community composition under two thermal regimes by means of a microcosm experiment. We chose the phanerogam *Myriophyllum spicatum*, more typical of meso-eutrophic habitats, and the charophyte *Chara hispida,* more frequent in oligotrophic waters and belonging to a much less studied macrophyte group, which, moreover, exhibit contrasting functional traits (i.e., roots versus rhizoids). The presence of both macrophyte types considerably reduced the diurnal diffusive CO_2 emissions due to their photosynthetic activity compared to bare-sediment situations. The radial oxygen loss of *M. spicatum* roots provided aerobic-microaerobic conditions beyond the first sediment centimeter, in contrast to more anoxic sediments created by *C. hispida*. As a result of this, each type of macrophyte determined a particular sediment microbiome. Despite dissolved CH_4 being greater in the presence of plants, no statistical differences in CH_4 diffusive flux caused by the presence or absence of plants was found. We demonstrated how the presence, or not, of macrophytes is more important than warming (in our case with a temperature difference of 3 °C) in relation to GHG emissions. Both species, being perennial, provide ecosystem services year-round and are strong candidates for management strategies aimed at transforming new or restored aquatic ecosystems into carbon sinks.

1. Introduction

Management approaches to mitigate and adapt to climate change might involve restoration efforts in inland waters such as giving rise to submerged vegetation meadows that contribute to the maintenance of, not only water in good condition (Su et al., 2019), but also to reduce emissions of greenhouse gasses (GHG). Therefore, in order to be more efficient when choosing species for restoration techniques such as reintroduction and translocation, the knowledge about the role of particular species of macrophytes regarding the emissions of GHG is of paramount importance (Bhushan et al., 2024; Hessen et al., 2024; Paranaíba and Kosten, 2024). Numerous studies have demonstrated that different macrophyte species in inland waters influence GHG emissions through distinct mechanisms and in different ways (Aben et al., 2022; Harpenslager et al., 2022; Gremmen et al., 2023; Theus et al., 2023; Schneider et al., 2024). For example, Schneider et al. (2024) recently demonstrated that macrophyte removal exerted variable effects on greenhouse gas emissions, depending on site conditions and plant life forms (main types: free-floating, submerged, emergent plants): for example, the removal of the floating-species *Pontederia crassipes* strongly increased CH_4 emission, particularly via ebullition, and the removal of the dominant primary producer *Elodea nuttallii* strongly reduced CO_2 fixation and increased CO_2 emission; albeit temporarily, helophytes and floating-species such as *Ranunculus* spp. can modify CH_4 emissions via plant-mediated transport. On the other hand, Aben et al. (2022) described how the response to warming was the strongest in

* Corresponding author.
E-mail address: maria.a.rodrigo@uv.es (M.A. Rodrigo).

https://doi.org/10.1016/j.jenvman.2025.125654
Received 6 March 2025; Received in revised form 18 April 2025; Accepted 1 May 2025
Available online 11 May 2025

free-floating plants and the weakest for submerged plant-dominated systems. In this sense, Ribaudo et al. (2023) also described how the colonization of free-floating forms increased emissions of GHG, mainly CH_4, in small freshwater wetlands. As can be seen, there is a lack of a universal response across case-study waterbodies, suggesting that both macrophyte life forms and environmental variables are very important factors determining final GHG emissions in inland waters.

As stated above, comparisons of GHG (CO_2, CH_4 and N_2O) emissions between different macrophytes already exist (Aben et al., 2022; Harpenslager et al., 2022; Ribaudo et al., 2023). The mechanisms by which macrophytes might affect GHG emissions are diverse (Bridgham et al., 2013; Benelli et al., 2020). Overall, CO_2 uptake is common to all types of macrophytes, but with different rates; however, the effect on CH_4 emission depends more on the macrophyte life form. Rooted macrophytes can oxygenize the sediments via high radial oxygen loss (ROL, O_2 transfer through aerenchyma by simple diffusion from well-oxygenated plant parts –leaves– to the hypoxic zones –roots, rhizomes–; Armstrong, 1964), thereby reducing methanogenesis and promoting CH_4 oxidation (Laanbroek, 2010). However, the roots might also act as a chimney for CH_4 emission (Bhullar et al., 2013). Floating forms reduce the gas exchange across the water-atmosphere interface (Attermeyer et al., 2016), which can reduce O_2 availability in the water column producing optimal conditions for methanogenesis, but the floating leaves can act as a trap for CH_4 bubbles, reducing methane emissions (Kosten et al., 2016). Moreover, aquatic plants affect the sediment microbial communities in different ways by altering, both chemically and physically, the features and properties of the sediment: O_2 enhancement, as stated above, and consequently modification of the redox potential, organic carbon release from root exudation (Karjalainen et al., 2001), among others.

A large fraction of the organic matter in the sediments in inland waters comes from the activity and senescence of macrophytes (Longhi et al., 2008), but not all macrophyte types are equally prone to degradation and, consequently, the transformation into GHG can also vary among species (Grasset et al., 2019; Wang et al., 2023). From our own research (Puche et al., 2025), we already know that cumulative CH_4 production was greater from detritus produced by freshwater macroalgae (such as the charophytes *Chara hispida* and *Nitella hyalina*) than from organic matter derived from vascular submerged plants (such as *Najas marina*, *Stuckenia pectinata* or *Myriophyllum spicatum*). Now, we want to focus on the effect of different functional traits of these macrophytes to understand their impacts on GHG emissions in future warmer waters, to provide new insights for adaptive management approaches, such as the reintroduction of macrophyte species in inland waters, for climate change mitigation and adaptation. Therefore, we have chosen *Myriophyllum spicatum* L. and *Chara hispida* L., which have distinct radicular systems (true roots *versus* rhizoids, respectively) and therefore might influence the oxic/anoxic conditions of the sediment differently, affecting the associated microbial community structurally and functionally, and consequently GHG emissions. The effects of submerged macrophytes on stimulating or depressing microbial processes (Benelli et al., 2020) via ROL, via the production of exudates or via the uptake of inorganic nutrients, for example, have been studied a lot more in vascular aquatic plants; however, the studies of these effects caused by macroalgae such as charophytes, dominant in particular types of lakes (*Chara*-lakes, Pukacz et al., 2016; habitat 3140 from the European Habitat Directive (Council Directive, 1992)) are almost absent. To fill this gap, we designed a laboratory experiment, to analyze the influence of *M. spicatum* and *C. hispida* on diffusive GHG (CO_2 and CH_4) emissions under two thermal regimes, focusing on the oxygen profiles formed in the water-sediment interface and the sediment at a millimetric scale, as well as the microbial community developed. We pose the following hypotheses: (i) the presence of macrophytes will reduce diurnal diffusive CO_2 emissions due to the photosynthetic activity compared to bare-sediment situations; (ii) the increased temperature will favor processes that can represent a higher GHG release, independently of the presence, or not, of macrophytes and their type; (iii) mechanisms such as ROL will be of greater importance for the vascular plant, therefore the higher O_2 content in the sediments will favor aerobic processes (such as nitrification, reduction of methanogenesis) and fewer GHG (particularly methane) will be emitted. The information obtained in our study will help to choose macrophyte species to develop management strategies in which conservation and restoration of inland waters are planned by involving macrophyte treatments to substantially mitigate GHG emissions in a context of global warming.

2. Material and methods

2.1. Experimental setup

An indoor microcosm experiment was performed using 18 cylindrical glass containers (diameter 15 cm, height 30 cm; capacity 5.3 L; Fig. S1). Plants, sediment, and water were collected on 8th January 2024 from two nearby (12 km away) oligo-mesotrophic ponds in Valencia (Spain): Mallada del Dosel, in Cullera (39° 12 ‘29″ N 0° 14’ 5″ W), where *Chara hispida* form dense meadows, and Tancat de l’Illa, in Sollana (39° 16′ 45″ N 0° 17′26″ W) where *Myriophyllum spicatum* thrives, also forming dense meadows. Both lagoons are located within a protected area (the Albufera de Valencia Natural Park).

Chara hispida L. is a robust and one of the largest charophyte species worldwide. It has often a greyish-green appearance due to incrustations. It is chiefly perennial and starts growing in spring from hibernating green plants or nodal fragments. The species can be found in a large variety of aquatic ecosystems, but mainly in standing water from oligo- to mesotrophic conditions. *Chara hispida* is a typical hard water species that can be found in shallow water (of about 50 cm depth) in small water bodies but also in lakes (occurring between 1 and 10 m). The species has been mainly recorded from Europe, from the Mediterranean Sea in the south to Scandinavia in the north, Estonia and Belarus in the east to the Iberian Peninsula in the west (Blindow et al., 2024). *Myriophyllum spicatum* L., the Eurasian watermilfoil, is a submerged, rooted, dicotyledonous, aquatic plant that can grow to more than 7 m long. It branches profusely once it reaches the surface and forms a dense canopy. It can live in different kinds of water bodies and is one of the species of the genus *Myriophyllum* that better resists eutrophic conditions, and absorb nutrients via both shoots and roots (Yu et al., 2016).

Plants were collected by means of a hook from the shore of both sides of each waterbody. Superficial sediment (the first 5 cm approximately) was collected by means of a shovel and kept in black plastic bags. Water was collected also from the shore using a 1.5 L-jar connected to a stick. Plants, sediments, and water were transported to the culture chamber inside a portable cooler in 1 h. Sediments from both origins were homogenized by thorough manual mixing before being added to each microcosm. Approximately 1.1 L of mixed sediment was added to each container, which constituted a layer of 5–6 cm. Since the containers were transparent, the 6-cm outer bottom part was covered with opaque tape to shade the sediment from the lateral side.

Each treatment was performed in triplicate ($n = 3$) to account for variability within the microcosm setup. While this replication level provides a basis for statistical comparisons, it is important to acknowledge that microcosms, by their nature, simplify environmental complexity. Consequently, caution should be exercised when extrapolating these findings to natural systems, where additional factors such as hydrodynamics, species interactions, and large-scale environmental heterogeneity may influence macrophyte-driven biogeochemical processes (Carpenter, 1996; Petersen et al., 2003).

The microcosms used for the plant treatments were planted with healthy, clean apical segments of the two different types of macrophytes (*M. spicatum* and *C. hispida*). Due to the different sizes of both species (*C. hispida* individual fresh weight: 0.62 ± 0.04 g; $n = 5$; *M. spicatum* individual fresh weight: 3.42 ± 0.38 g; $n = 5$) each *Chara* incubator was stocked with 36 individuals and each *Myriophyllum* incubator with 6 individuals. This resulted in a different plant density (2037 individuals/

m^2 for *Chara* and 340 individuals/m^2 for *Myriophyllum*), but a similar initial biomass (21–22 g FW per incubator; 1188–1245 g FW/m^2). After the introduction of the sediment and the plants, the microcosms were filled to almost the top of the incubator (3.9 L) with dechlorinated tap water (final conductivity 1.2 mS/cm). Moreover, 10 mL of water from each pond was added to each microcosm to provide the inoculum of natural microorganisms. Finally, 5.82 mL of a concentrated nitrate solution (1000 mgN/L) were added to each incubator (1.5 mg/L final concentration). Six incubators were treated in the same way, but without plants as controls. Then, all the incubators were left to acclimate for 13 days before the experimental warming (see below). The microcosms were maintained in a controlled environment (culture room) at approximately 21 °C, and illuminated using Sylvania Gro-Lux F58W tubes which provided 200 μmol photons/m^2·s at the water-surface layer of the incubators. The light/dark cycle was around 14 h of daylight and 10 h of darkness (simulating early summer conditions). To avoid the "site effect" the position of the incubators was changed every two days. Some extra containers were set to measure some particular variables (i.e., oxygen microprofiles in the sediment at the beginning of the experiment; see section 2.2.6).

Temperature treatments consisted of a lower and more variable temperature (mean 21 ± 1 °C), trying to mimic a temperate scenario, and a warmer and more constant temperature (mean 24 ± 0.4 °C), trying to resemble a more "tropical" scenario. The latter temperature treatment of an increase of approximately +3 °C is also consistent with the predicted warming by 2050 in Europe under anthropogenic GHG emissions between scenarios SSP2-4.5 and SSP3-7.0 (IPCC et al., 2023). The outlined scenarios anticipate significant warming in inland water bodies, which will affect thermal water stratification, species distribution and biogeochemical cycles. Freshwater ecosystems are particularly vulnerable to such changes, as even moderate temperature rises can disrupt, for example, macroinvertebrate communities, alter microbial activity and accelerate GHG emissions from sediments (CORDIS, 2015; Woodward et al., 2010; Kraemer et al., 2017). To achieve the increase in temperature, the incubators were placed inside rectangular plastic containers (24x30 × 16 cm; 11.5 L) filled with tap water (two incubators per container). Half of these containers were provided with Eheim Jäger 25 W aquarium heaters to keep the higher and more constant temperature in the warmer scenario. Throughout the experiment, the microcosms were gently refilled with a mixture of demineralized and tap waters once or twice per week to compensate for evaporation losses. The experiment lasted a total of 42 days.

2.2. Measured variables

2.2.1. Diffusive greenhouse gas fluxes

Direct measurements of GHG total evasion fluxes (FCO_2, FCH_4) from the air-water interface were performed weekly using a home-made, plastic gas chamber (diameter: 15 cm; volume: 3.5 L) tightly located in the upper part of the microcosms and connected in a closed loop to a greenhouse gas analyzer (Gasera ONE PULSE) based on photoacoustic spectroscopy through NDIR-PAS technology (mechanically chopped broadband IR source with optical bandpass filters) (Vargas-Sánchez et al., 2023). Each measurement ran for 40 min. The diffusive CO_2 and CH_4 fluxes were determined from the slope of the change in the gas concentration (ppm; ΔC) inside the chamber concerning the sampling time (Dt; s) by means of linear regression. The area (Ac; m^2) and the volume (Vc; m^3) of the chamber were also considered [$F_{gas} = (\Delta C/\Delta t)^*$ (Vc/Ac)]. The concentrations were adjusted for pressure and temperature according to the ideal gas law (Vargas-Sánchez et al., 2023) and expressed as mg of gas/m^2·h.

2.2.2. Dissolved greenhouse gas concentrations

Dissolved GHG concentrations were measured using the headspace equilibration technique, avoiding the acidification of the water sample, as described by Goldenfum (2010). Forty milliliter water samples (in triplicate) were taken at two depths (above the sediment and close to the surface of the incubators) by means of 50-mL plastic syringes. Helium gas (20 mL) was incorporated into each syringe and then they were vigorously shaken for 3 min to transfer the helium to the water and the CO_2 and CH_4 to the headspace. The 20-mL of air in the headspace of the three replicates was transferred to another syringe. The integrated 60-mL air volume was introduced into the greenhouse gas analyzer described above, and CO_2 and CH_4 concentrations were quantified and also adjusted for pressure and temperature according to the ideal gas law (Vargas-Sánchez et al., 2023). The dissolved gas concentrations were expressed as mg of gas/L.

2.2.3. Water temperature, pH, dissolved oxygen and sestonic chlorophyll *a*

Water temperature, pH, dissolved oxygen and chlorophyll *a* were measured in each microcosm twice per week. A Hach oximeter was used to measure oxygen, and the pH was measured with a Crison Basic 20 pH-meter. The temperature was measured with the oximeter device in each incubator, and in addition four Onset HOBO (UA-002-64) sensors were located in one incubator of each treatment to record temperature continuously. In vivo chlorophyll *a* was measured using an AquaFluor (Turner Designs) fluorometer and further calibration with the pigment extraction-spectrophotometer method (Rodrigo and Segura, 2020).

2.2.4. Water chemical analyses

Nitrate, nitrite, ammonium, dissolved organic and inorganic carbon were measured at the start (day 16), mid-term (day 30) and the end (day 42) of the experiment. $N\text{-}NO_2$, $N\text{-}NO_3$ $N\text{-}NH_4$ analyses were performed in a Slar Sanplus System segmented flow autoanalyzer following standard methods (Vargas-Sánchez et al., 2023). Total dissolved inorganic carbon (DIC) was determined after filtering 60 mL of the water sample through Whatman GF/F filters which were then acidified with H_3PO_4 (85 %). The DIC samples were stored in a cold, dark place for 24 h to force the equilibrium of the carbonate system. Then the CO_2 gas was extracted using the headspace technique and stored in 12 mL Exetainer vials (Labco) previously evacuated until analyses. The dissolved CO_2 concentration was also measured using the headspace equilibration technique, avoiding the acidification of the water sample, as described by Goldenfum (2010). Then the CO_2 was transferred into Exetainer vials (12 mL) for subsequent analysis. All samples were analyzed by gas chromatography (Agilent model 6890N) equipped with a single-stage dual-packed column, where CO_2 was detected using a thermal conductivity detector.

2.2.5. Plant abundance at the end of the experiment and growth rate

Final macrophyte abundance was measured by removing all the specimens from the sediment and cleaning and drying them in a desiccation oven (70 °C, 24 h). Later, they were weighed using an OHAUS Scout scale (0.01 g). The well-developed root system of *M. spicatum* was separated from the sediment, and from the rest of the plant, and weighed separately from the above-ground plant. However, it was impossible to obtain and separate the delicate rhizoidal system of *C. hispida* from the sediment, therefore, only above-ground biomass was considered for the charophyte. The biomass of *C. hispida* was corrected by detracting the content of carbonate in the external incrustations that this species accumulates (30 % of total biomass, based on annual means; Rodrigo et al., 2015). Growth rates were calculated on macrophyte biomass considering an exponential growth model (Van den Berg et al., 2002).

2.2.6. Profiles of oxygen at millimetric scale in the sediments

Dissolved oxygen (DO) microprofiles were obtained from the water-sediment interface to the 1–2 cm sediment layer in each incubator at the end of the experiment (and in extra incubators at the beginning of the experiment). To do this, a transparent methacrylate core (diameter 4 cm, height 15 cm) was used to isolate the samples from each incubator, being careful not to disrupt the water-sediment interface. The cores were vertically placed on a stable platform (Unisense, Denmark). The DO was

measured with an oxygen Clark-type microelectrode (5 μm tip diameter) (Unisense, Denmark). The microelectrode was previously calibrated following the manufacturer's instructions. The signal from the microelectrode was recorded using a Microsensor Multimeter (Unisense, Denmark) linked to a computer. The DO measurements were carried out every millimeter using a micromanipulator (Unisense, Denmark) that allows you to accurately set the tip of the microelectrode to the desired position.

2.2.7. Microbial community in the sediments

Sediment samples (c.a. 0.25 g of fresh weight), used for DNA extraction (PowerSoil® DNA Isolation Kit, Qiagen) and sequencing, were collected (at the start –prior to planting- and at the end of the experiment) by means of a sterilized spatula in 1-mL Eppendorf tubes at two different depths of the sediment profile (superficial: 0–1 cm, and sub-superficial: 1–2 cm) in one of the replicate incubators for each treatment (for initial time), and in the replicate incubators for each treatment. The tubes were stored at −80 °C until analyzed by the Genomic Section of the Central Service for Experimental Research (SCSIE) of the University of Valencia. 16S rDNA V4 region amplification was performed using the primers described in Caporaso et al. (2012), following a two-step PCR. In the first step, a specific primer against 16S v4 region was selected and overhang adapter sequences appended for compatibility with Illumina indexes and sequencing adapters. After amplification, PCR cleanup was carried out with magnetic beads, and purified fragments were used in a second PCR using a limited number of cycles and Nextera XT adapter primers (Illumina). Clean up of final libraries was performed with magnetic beads. The quantity and size of each library were checked with the Fragment Analyzer HS NGS Kit (Agilent). Sequencing was performed on MiSeq instrument (Illumina, USA) using paired 251-bp reads, and MiSeq v2 reagents. The ends of each read were overlapped to generate high-quality, full-length reads of the V4 region. Sequencing data were demultiplexed using the Illumina bcl2fastq© program. Demultiplexed paired FASTQ sequences were imported into the QIIME2 platform for read preprocessing and microbiome analysis. Quality control was carried out using the DADA2 pipeline incorporated into QIIME2 (Caporaso et al., 2010). The DADA2 program filtered out phiX reads, removed chimeric sequences and assigned reads into Amplicon Sequence Variants (ASVs) (Callahan et al., 2016). Taxonomic annotation was obtained using the SILVA v138 database.

The results were reported as the number of sequences (hits) obtained and the percentage of sequences from each OTU in each sample. For each sample, we selected OTUs with more than 300 hits, or 0.1 % of total hits. We decided to consider the phyla and family matrix due to the large number of genera and species detected, and these are more trustworthy than those of species level (Fox et al., 1992; Azua-Bustos et al., 2018). For the comparative analysis of sample composition in the different sediment layers and treatments, we used two datasets: one with phyla which represented more than 1 % of hits, and a second one with families which had more than 1 % of hits.

The bacterial and archaeal data are deposited in https://zenodo.org/records/14976594 for public access.

2.2.8. Diversity and community structure

The Shannon index was used as an alpha-diversity estimator for the sediment microbial community. The index was calculated for bacterial and archaea communities separately (on phyla and on families in both cases) at the beginning and the end of the experiment at superficial and sub-superficial sediment layers. Beta-diversity based on community structure was assessed by calculating a pairwise Bray-Curtis dissimilarity distance matrix for each microbial community in both sediment layers at the end of the experiment, and to compare the changes in the community structure between initial and final time for each treatment.

2.3. Statistical analyses

Generalized additive models (GAMs) (Wood, 2006) were used to assess the differences among the treatment trends of GHG fluxes and water concentration in the microcosms throughout the days of the experiment. GAMS are particularly useful for estimating linear, nonlinear, and non-monotonic relationships between response variables and predictors, even when predictors are categorical and not continuous values (Wood et al., 2016; Webb et al., 2019). All GAMs model coefficients were estimated using restricted marginal likelihood (REML) with the mgcv package (Wood, 2011; Wood et al., 2016). Post-hoc analysis using estimated marginal means (EMMs) were used to differentiate among plant and temperature treatments from GAM models. EMMs provide an adjusted mean estimate for each treatment level while accounting for the model's fixed effects (Lenth, 2016). EMMs for each treatment and the performed pairwise comparisons with Bonferroni correction to control for multiple testing were obtained. This analysis was performed using the emmeans package (Lenth, 2023). Different ANOVA approaches were used depending on the specific variable. A one-way ANOVA was used to assess differences in final macrophyte biomass and growth rate between *Chara* and *Myriophyllum* treatments. A similar approach was used for the Shannon index and beta-diversity among conditions. Two-way ANOVAs (plant × temperature) were conducted to evaluate differences in dissolved oxygen at the water-sediment interface across treatments. Three-way ANOVAs (plant × temperature × time) were performed to analyze pH, dissolved O_2, microalgal chlorophyll *a* and nutrient concentrations in the water column in the microcosms over time. When significant differences were detected, Tukey's post hoc tests were applied to determine pairwise differences between treatments. A Principal Component Analysis (PCA) using the standardized relative abundance data was performed to explore the multivariate patterns in bacterial and archaeal community composition. The PCAs were conducted separately for bacterial and archaeal communities as well as for superficial and sub-superficial sediment layers. An analysis of variance using the function Adonis from the vegan package was performed to verify if there were differences among the treatments shown in the different PCAs. Finally, linear regressions by plant treatment were performed to assess the variables influencing gas production with data of water physical and chemical variables and bacterial and archaeal communities. The linear regressions were performed using the average values of the last three measurement days for gas production and the last four measurements of chemical variables. All analyses were performed using the R programming language (version 4.4.1; R Core Team, 2024). Significant statistical differences were considered when $p < 0.05$.

3. Results

3.1. CO_2 and CH_4 diffusive fluxes

Non-vegetated incubators acted as CO_2 sources, with fluxes varying between 8.8 and 40.8 $mgCO_2/m^2 \cdot h$ (Fig. 1A). Bare sediment treatment differed significantly from *Myriophyllum* and *Chara* treatments ($p < 0.001$). Close to the end of the experiment, the flux of emitted CO_2 was higher in the lower temperature treatment, although the differences were not statistically significant among Bare Sediment scenarios. Conversely, incubators with vegetation showed negative CO_2 fluxes at all moments (Fig. 1A), acting as gas sinks and being significantly different between them ($p = 0.002$). The highest sink values were registered in the *Myriophyllum* treatment in the lower temperature scenario, which was statistically different from all the other vegetation and temperature treatments ($p = 0.015$). For the *Chara* treatment, the value range was −5 $mgCO_2/m^2 \cdot h$ and −70 $mgCO_2/m^2 \cdot h$, and for the *Myriophyllum* treatment it was −20 $mgCO_2/m^2 \cdot h$ and −99 $mgCO_2/m^2 \cdot h$.

The CH_4 emission fluxes (Fig. 1B) remained positive but low throughout the experiment, on most occasions lower than 0.05 $mgCH_4/m^2 \cdot h$. Only in the initial moments of the experiment did the

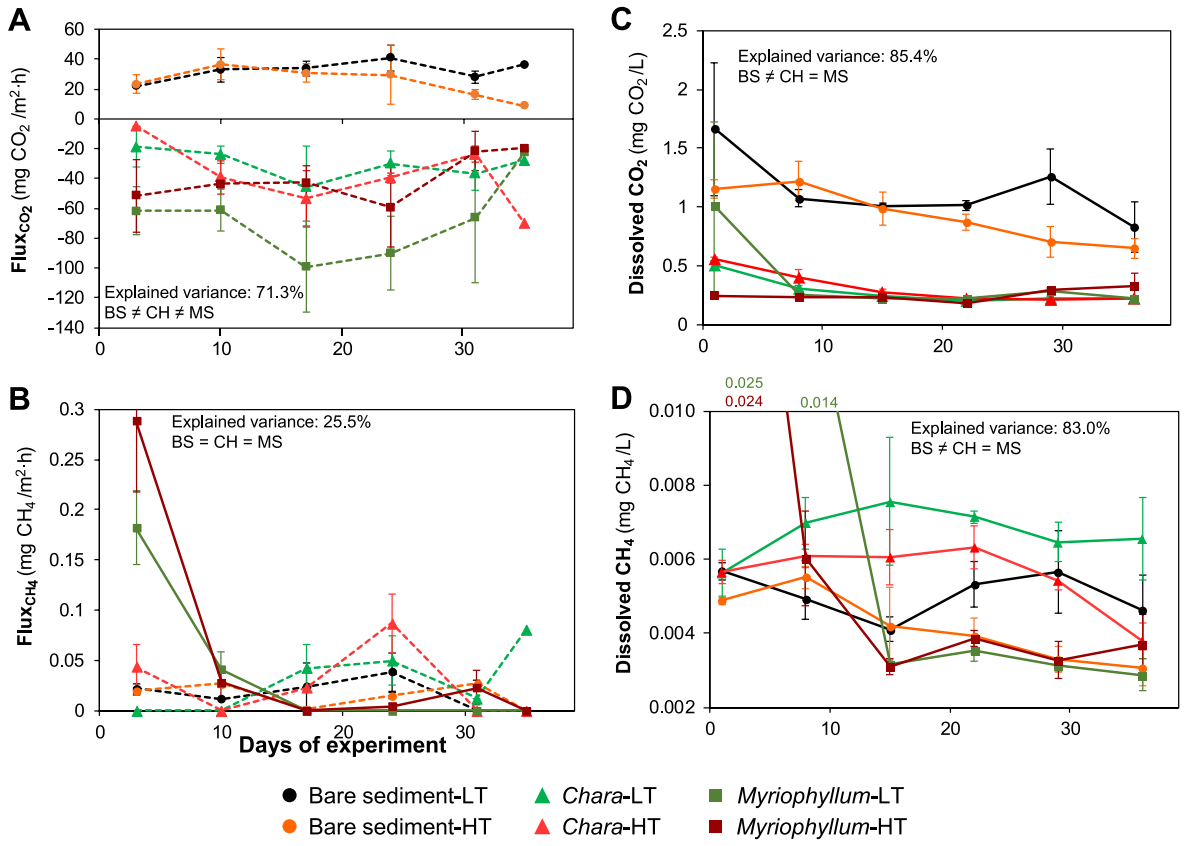

Fig. 1. Dynamics of the emission fluxes of CO_2 (**A**) and CH_4 (**B**), and dissolved concentrations of CO_2 (**C**) and CH_4 (**D**) throughout the experiment under the different experimental conditions of macrophytes (bare sediment as control (BS), *Chara hispida* (CH) and *Myriophyllum spicatum* (MS)) and of temperature (LT: lower temperature; HT: higher temperature). The percentage of explained variance of the generalized additive model (GAM) is expressed for each variable as well as the significant differences among the types of macrophytes (since the temperature treatment had no significant effect). Dotted lines represent no significant differences among the days of experiment. Vertical bars indicate standard errors.

Myriophyllum treatment show values around 0.25 mgCH_4/m^2·h; however, no statically significant differences caused by temperature treatment or type of macrophyte were found. Moreover, CH_4 emission fluxes had the lowest explained variance (25.5 %) of all the GAM models.

3.2. Dissolved CO_2 and CH_4 concentrations

As happened with the gas emissions, the concentration of dissolved CO_2 was significantly higher in the Bare-sediment treatment compared to the macrophyte treatments ($p < 0.001$) (Fig. 1C). A significant declining trend in CO_2 concentrations was observed throughout the experiment in the Bare-sediment treatment ($p < 0.001$). The different types of macrophyte did not produce significant differences in dissolved CO_2, but, again, a significant declining trend was registered over time ($p < 0.001$), changing from 0.6 ± 0.2 mg/L at initial dates to 0.2 ± 0.0 mg/L at the end of the experiment.

The dissolved CH_4 concentrations showed a similar pattern in comparison to the diffusive flux of this gas, with higher concentrations (0.024 ± 0.004 mgCH_4/L) in the *Myriophyllum* treatments (both the lower and higher temperatures) at the beginning of the experiment which reduced considerably later on (Fig. 1D). The CH_4 concentrations in the Bare-sediment treatment were lower and statistically different compared to the values of plant treatments ($p < 0.001$). While, considering only the macrophyte treatments, the CH_4 concentrations between *Chara* and *Myriophyllum* treatments were not statistically different (Fig. 1D). The explained variance of GAM models for CH_4 and CO_2 concentrations were quite similar (85.4 % and 83.0 %, respectively) and indicated that the *Chara* and *Myriophyllum* treatments had a similar trend, but differed from the Bare-sediment treatment (Fig. 1C and D).

3.3. Water chemical properties and sestonic chlorophyll *a* concentration

The water pH and the dissolved oxygen concentrations were significantly lower in the Bare-sediment treatments and remained more or less constant throughout time (around 8 (Fig. 2A) and 9 mgO_2/L (Fig. 2B), respectively). The water pH in the treatments with vegetation increased with time, particularly in the *Myriophyllum* treatment, and the oxygen concentrations reached more than 15 mgO_2/L on many occasions in said treatment. Water pH was statistically higher at the lower temperature. The sestonic chlorophyll *a* concentrations were low in all treatments, always below 4 μg/L, and usually below 2 μg/L (Fig. 2C). The highest values were found in the *Myriophyllum*-HT treatment, particularly on day 10 of the experiment, but decreased later on. Higher temperature conditions caused statistically significant larger chlorophyll *a* concentrations.

The nitrogen forms, particularly nitrate and nitrite concentrations were statistically higher in the Bare-sediment treatment (Fig. 2D and E) and both contents decreased significantly with time. In particular, in the *Chara* treatments the nitrate and nitrite concentrations were reduced by 67 % and 82 %, respectively. Overall, temperature did not have a significant effect on the nitrate concentrations. Ammonia concentrations were also higher in the Bare-sediment treatment (Fig. 2F); however, a decline over time was not observed. Total nitrogen (Fig. 2G) followed the same patterns as that of nitrate. Phosphate concentrations (Fig. 2H) were slightly different on day 15 of the experiment among treatments (ranging from 0.0010 ± 0.0003 mg P/L in Bare-sediment-HT to 0.391 ± 0.379 mg P/L in *Myriophyllum*-LT), and they were undetectable at the middle and final times. Total phosphorus (Fig. 2I) showed the same pattern of soluble P, and the concentration was higher in the

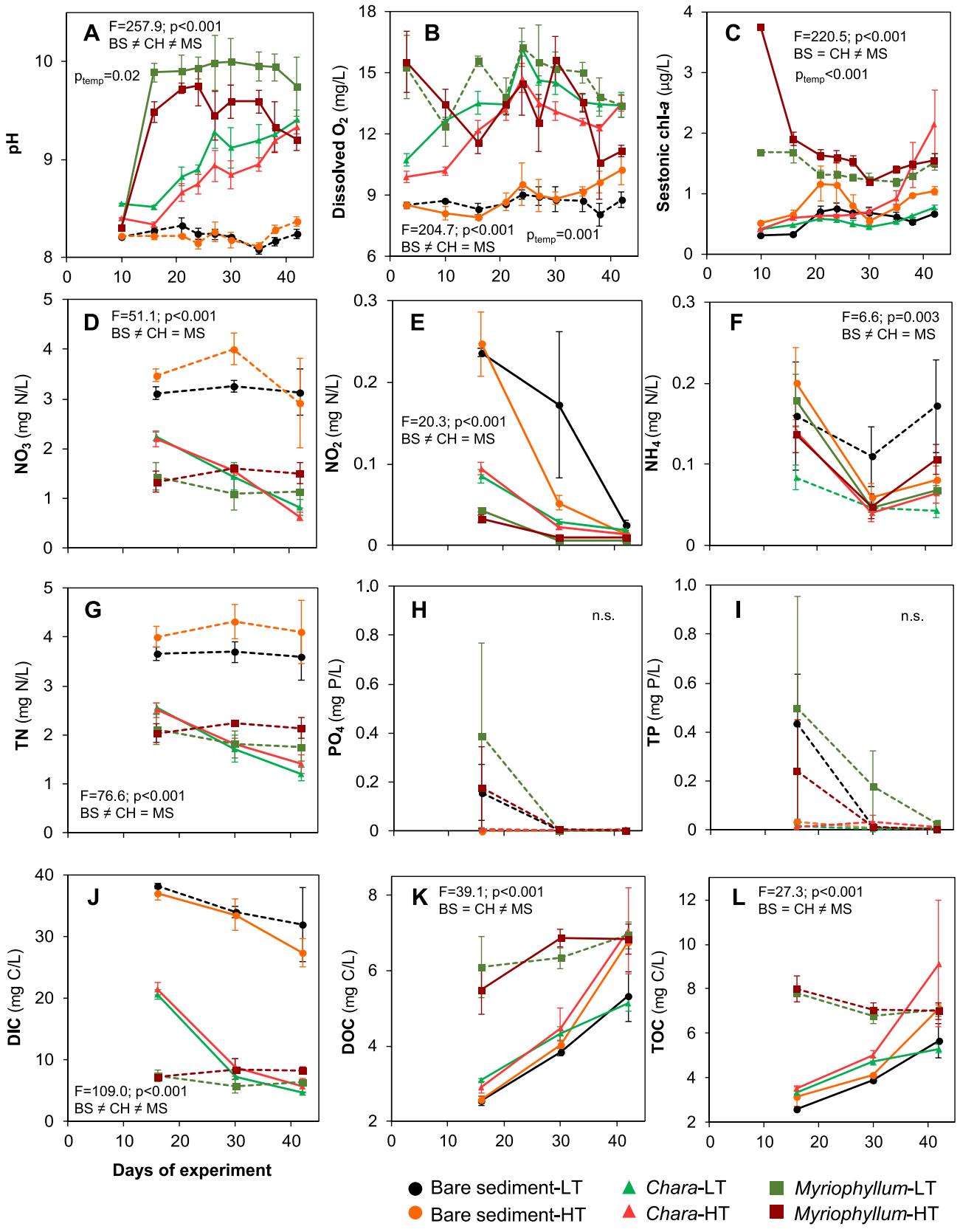

Fig. 2. Dynamics of water chemical variables and sestonic chlorophyll *a* throughout the experiment under the different experimental conditions of macrophytes (bare sediment as control (BS), *Chara hispida* (CH) and *Myriophyllum spicatum* (MS)) and of temperature (LT: lower temperature; HT: higher temperature). The F-statistic and p-value obtained with 3-way ANOVA for the significant effect of the type of macrophyte (as well as the differences obtained with the Tukey post-hoc analysis) are expressed for each variable. The effect of temperature considering all treatments together was only significant in water pH, dissolved oxygen and sestonic chlorophyll *a* (p-value showed in the graphs). Dotted lines represent no significant differences among the days of experiment. Vertical bars indicate standard errors. n.s.: non-significant.

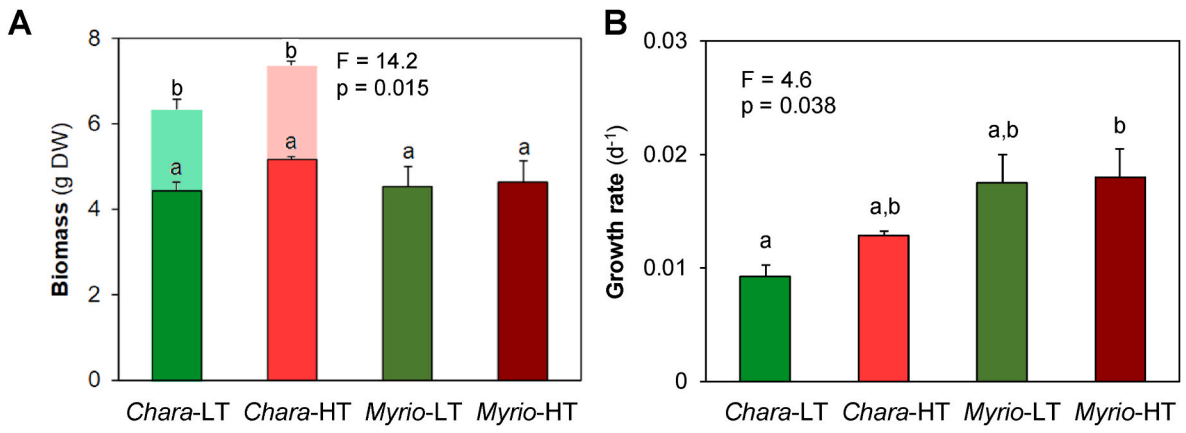

Fig. 3. **A:** Final macrophyte organic biomass at the end of the experiment. For *Chara hispida*, the darker part of the bars represents the biomass without the content of calcium carbonate of the incrustations, while the lighter parts represent the whole biomass considering also the calcium carbonate content. **B:** Macrophyte growth rate based on organic biomass data. ANOVA F and p-values are shown on each graph. Lower-case letters indicate significant differences within treatments after the Tukey post-hoc test. In the biomass graph the F and p correspond to the total biomass comparison among treatments.

Myriophyllum-LT treatment.

Dissolved inorganic carbon (DIC) concentrations were significantly much higher in the Bare-sediment treatment compared to the macrophyte treatments (Fig. 2J); they decreased over time (from 37.6 ± 0.6 mg/L at the beginning of the experiment to 29.7 ± 3.1 mg/L at the end), but they were not affected by the temperature scenario. For the plant treatments, initially, the DIC concentration was statistically higher in the *Chara* treatment, but over time the DIC content in both macrophyte treatments almost tallied. Neither temperature showed significant effects on DIC. Conversely, dissolved organic carbon (DOC) concentrations were higher in the macrophyte treatments in comparison to the Bare-sediment treatment (5.5 ± 0.3 mg C/L versus 4.0 ± 0.4 mg C/L) (Fig. 2K), and the DOC in the *Myriophyllum* treatment (6.4 ± 0.2 mg C/L) was statistically higher than in the *Chara* treatment (4.5 ± 0.4 mg C/L). In all cases, DOC significantly increased over time. The total organic carbon (TOC) concentrations (Fig. 2L) followed a similar pattern to those of DOC.

3.4. Macrophyte biomass and growth rate

Mean *M. spicatum* biomass at the end of the experiment was 4.6 ± 0.3 gDW and there were no statistical differences between the temperature treatments (Fig. 3A) nor with the final biomass of *C. hispida* (4.8 ± 0.2 gDW) considering only the organic part. The shoot/root ratio in *M. spicatum* ranged between 2.2 and 4.3, but there were no significant differences between temperature treatments ($p = 0.118$). The mean growth rate based on organic weight ranged between 0.009 and 0.018/d and the only significant differences were found between the *Chara* treatment-LT and the *Myriophyllum* treatment-HT ($p = 0.038$) (Fig. 3B).

3.5. Microprofiles of O_2 in the sediment

At the start of the experiment, the O_2 concentration at the water-sediment interface was 4.0 mgO_2/L and it was almost undetectable from 5 mm (Fig. 4). At the end of the experiment, the dissolved oxygen concentration at the water-sediment interface was similar when comparing macrophyte presence or absence (4.2 ± 0.8 mgO_2/L, mean

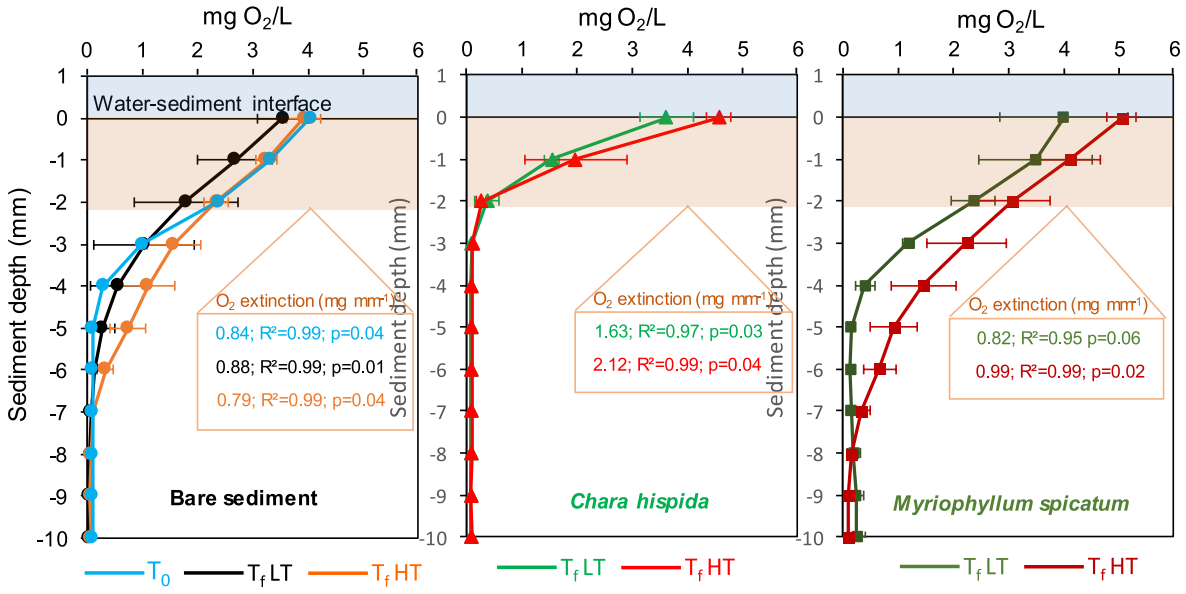

Fig. 4. Vertical profiles of dissolved oxygen at a millimeter scale within the first centimeter of sediment across the different macrophyte treatments and temperature conditions at the end of the experiment. For microcosms without vegetation, data from the initial time are also included. Horizontal bars indicate the standard errors of the three replicates per condition. The rate of O_2 depletion in the upper 2 mm of sediment is also shown.

± standard deviation), but the higher temperature treatments, when macrophytes were present, had slightly higher oxygen content at the interface ($p = 0.02$). In the first 2 mm of depth, the oxygen extinction rate was two-fold faster in the *Chara* treatment than in the *Myriophyllum* treatment, and the later was similar to the values found in the Bare-sediment treatment. At a depth of 3 mm in the sediment almost no oxygen (<0.1 mg/L) was detected in the *Chara* treatment, while 1.7 ± 0.7 mg/L and 1.3 ± 0.4 mg/L were measured in the *Myriophyllum* and Bare-sediment treatments, respectively (Fig. 4).

3.6. Sediment microbial community

Through high-throughput sequencing, a total of 6,215,656 sequences from all the samples were obtained (including initial and final time samples and superficial and sub-superficial samples from all conditions). After the implementation of all quality control criteria described above, 5,421,053 sequences (87.2 %) were retained for further analysis. The average number of sequences per sample was 147,992. Out of all sequences, less than 1 % belonged to Archaea. The highest number of sequences by plant treatment were detected in *Chara*, followed by Bare-sediment and *Myriophyllum* (Fig. S2–A), and, considering the condition, the order was *Chara*-HT > Bare Sediment-LT > *Myriophyllum*-HT (Fig. S2–B).

The analyses detected 4517 OTUs belonging to 86 phyla, 830 families and 1362 genera in total. The bacterial community was composed of 74 phyla, 781 families and 1305 genera. There were 187 Archaea OTUs, which represented 4.1 % of all the OTUs. The Archaea community was represented by 12 phyla (plus one "uncultured"), 49 families and 57 genera.

Neither bacterial phyla nor families exclusive for a particular treatment were detected, only the representation changed (Figs. 5 and 6). In all conditions, in both sediment layers and at both times, considering all the OTUs, 14 phyla were obtained (more than 1 % representation), and the Proteobacteria phylum was the most abundant (37.6 ± 7.6 %) followed by Bacteroidota (18.7 ± 2.6 %), Desulfobacterota (11.9 ± 3.1 %) and Verrucomicrobiota (7.4 ± 1.6 %) (Fig. 5).

Bacterial families representing more than 1 % were affiliated to six phyla. The most represented family was Hydrogenophilaceae (Proteobacteria, 19.4 ± 3.9 %) followed by Desulfosarcinaceae (Desulfobacterota, 11.1 ± 2.8 %), Bacteroidetes_vadinHA17 and Microscillaceae (Bacteroidota, 6.7 ± 2.4 % and 6.5 ± 5.6 %, respectively) and Pedosphaeraceae (Verrucomicrobiota, 6.3 ± 1.0 %) (Fig. 6; Table S1).

Regarding Archaea, and similar to the bacterial community, no exclusive phyla OTU was detected for any particular treatment/condition, but their representation also changed (Fig. 7). Within Archaea, 13 phyla were considered (more than 1 % representation). Nanoarchaeota was the most represented phylum (41.4 ± 11.0 %) followed by Crenarchaeota (23.9 ± 10.7 %) and Thermoplasmatota (14.8 ± 5.9 %). Archaeal families representing more than 1 % were affiliated to seven phyla. Woesearchaeales was the most represented family (27.6 ± 9.0 %) followed by Bathyarchaeia (18.2 ± 7.5 %), OTUs which did not correspond to any cultured family (12.4 ± 4.0 %), and Marine Benthic Group D and DHVEG-1 (8.4 ± 3.8 %) (Fig. 8; Table S2).

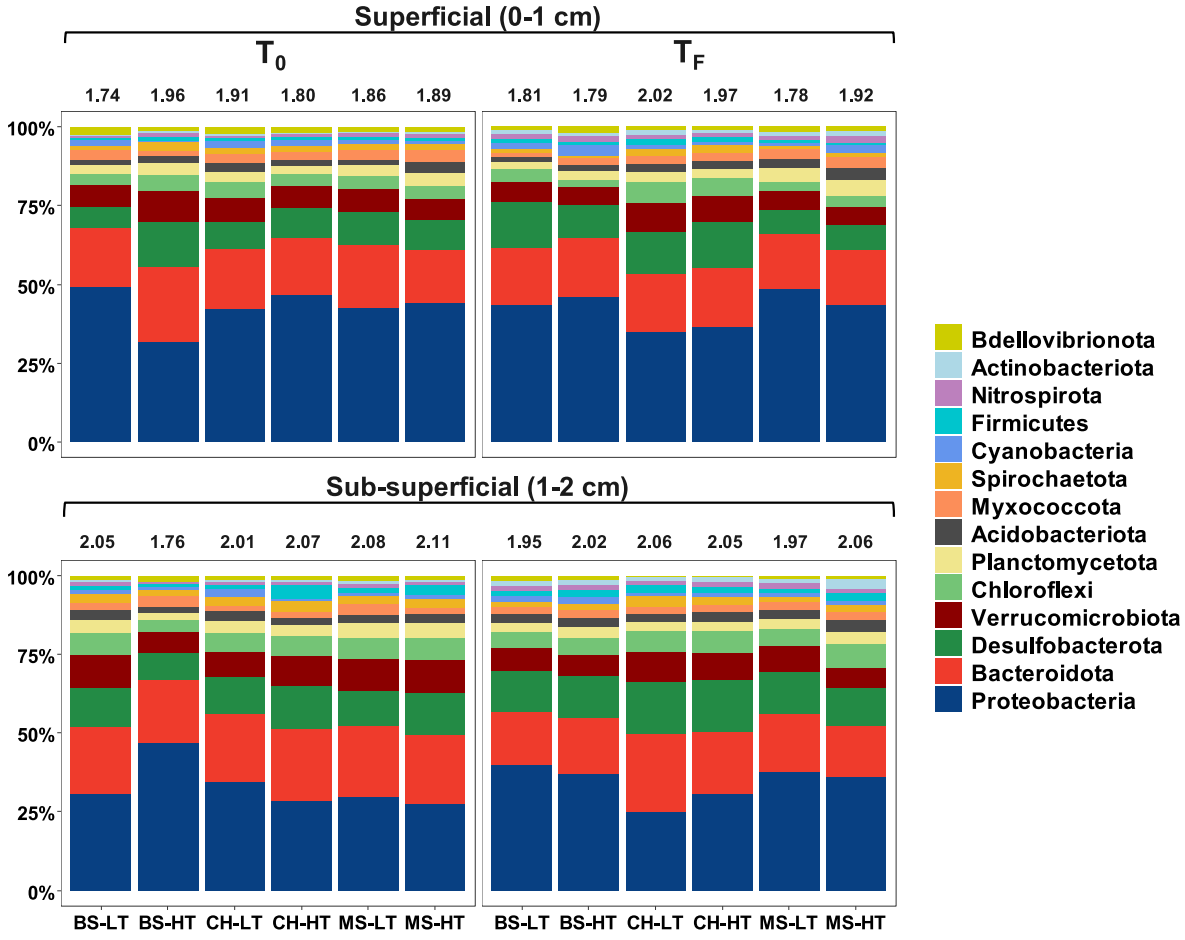

Fig. 5. Barplots of relative abundance of OTUs corresponding to bacterial phyla in the sediment microbial community in the different conditions of each treatment in both layers of sediments (superficial: 0–1 cm, sub-superficial: 1–2 cm) and before planting (T_0) and at the end of the experiment (T_F). Bare sediment (BS), *Chara hispida* (CH) and *Myriophyllum spicatum* (MS); LT: lower temperature; HT: higher temperature. Numbers above each condition column indicate the average of Shannon index values (bits) of the three replicates of each condition.

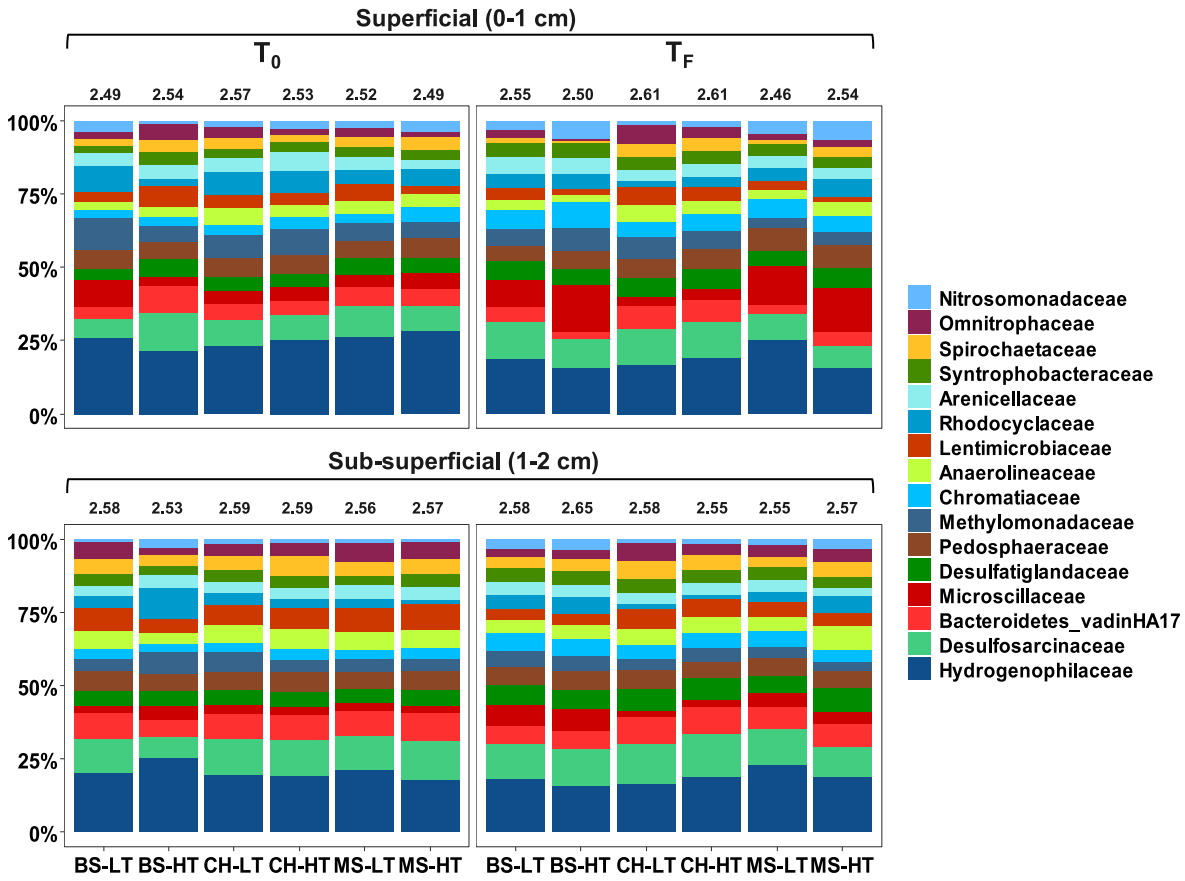

Fig. 6. Barplots of relative abundance of bacterial families in the sediment microbial community in the different conditions of each treatment in both layers of sediments (superficial: 0–1 cm, su-superficial: 1–2 cm) and before planting (T_0) and at the end of the experiment (T_F). Bare sediment (BS), *Chara hispida* (CH) and *Myriophyllum spicatum* (MS); LT: lower temperature; HT: higher temperature. Numbers above each condition column indicate the average of Shannon index values (bits) of the three replicates of each condition.

The microbial community structure at initial time comparing the different conditions was not statistically different. The largest change in the bacterial community structure comparing the initial and final times was found in the superficial (0–1 cm) sediment layer in comparison to the sub-superficial one (mean Bray Curtis distance between T_0 and T_F based on family composition: 0.23 vs 0.16, respectively, $F_{ANOVA} = 5.9$, $p = 0.036$; Table S3). However, the changes experienced by the Archaeal community with the incubation time were of the same order in both sediment layers (0.25 vs 0.22, respectively, $F_{ANOVA} = 0.5$, $p = 0.514$; Table S2). In particular, in the *Chara*-treatment, in the superficial sediment layer, there was a decrease in the Proteobacteria phylum representation (from 43.5 % to 35.4 %) (Fig. 5), impacting on the increase in the alpha-diversity values (from 1.7 to 1.8 bits in T_0 to 1.9–2.1 bits in T_F; Fig. 5). Regarding the Archaea, there was a decrease in the phylum Nanoarchaeota in favor of Crenarchaeota in both sediment layers (Fig. 7); however, the beta-diversity values, comparing the initial community with the final community at the family level among conditions (Table S3), were only statistically different ($p = 0.032$) for *Chara*-treatment-HT, which was lower in comparison to Bare-sediment-HT (Bray Curtis distance: 0.15 vs 0.44) for the superficial sediment layer.

Considering all the conditions together, the PCA analyses of both bacterial phyla and families (Fig. S3A–B) showed differences in the bacterial community distribution between superficial and deeper sediment layers, with Nitrospirota, Proteobacteria and Cyanobacteria phyla mainly represented in the superficial layer, and Chloroflexi, Spirochaetota, Verrumicrobia and Desulfobacterota in the sub-superficial layer. In terms of bacterial families, Microscillaceae, Nitrosomonadaceae and Rhodocycladaceae were mainly associated with the superficial layer. Regarding Archaea phyla and families (Fig. S3C–D), the separation between sediment layers was also significant although less evident.

Considering the superficial sediment layer separately (Fig. 9A and B), the plant treatment clearly influenced the bacterial community distribution. There was a clear separation of phyla depending on the existence or not of plants, but also depending on the plant treatment (*Chara* versus *Myriophyllum*) (Fig. 9A). The phyla associated with the Bare-sediment treatment were Proteobacteria, Cyanobacteria and Bacteroidota, while in the *Chara* treatment, the main related phyla were Desulfobacterota, Verrumicrobiota, Spirochaetota and Chloroflexi, and for the *Myriophyllum* treatment they were Acidobacteriota, Myxococcota Planctomycetota and Nitrospirota. At a family level (Fig. 9B), mainly Rhodocyclaceae, Nitrosomonadeceae, Microscillaceae and Chromatiaceae were associated with the Bare-sediment treatment, and Lentimicrobiaceae, Desulfatiglandaceae, Bacteriodetes_vadinHA17, Anaerolineaceae, Omnitrophaceae and Spirochaetaceae with the *Chara* treatment. In the sub-superficial sediment layer (Fig. 9C and D), the separation of bacterial phyla and families, although significant, was not as evident as in the superficial layer.

For Archaea, the phylum associated with the Bare-sediment treatment in the superficial sediment layer (Fig. 9E) was mainly Halobacterota. Thermoplasmatota, Micrarchaeota, Hadarchaeota and Iainarchaeota were the phyla associated with the *Chara*-treatment, while Crenarchaeota was mainly associated with the *Myriophyllum*-treatment. Regarding the families in the superficial sediment (Fig. 9F), a family of Woesearchaeales, Methanoregulaceae and Nitrosphaeraceae were related to the Bare-sediment treatment; Methanosaetaceae, Methanofastidiosaceae and a family of Micrarchaeales, a family of SG8-5C and GW2011 with the *Chara*-treatment; GW2011_GWC1_47_15 and

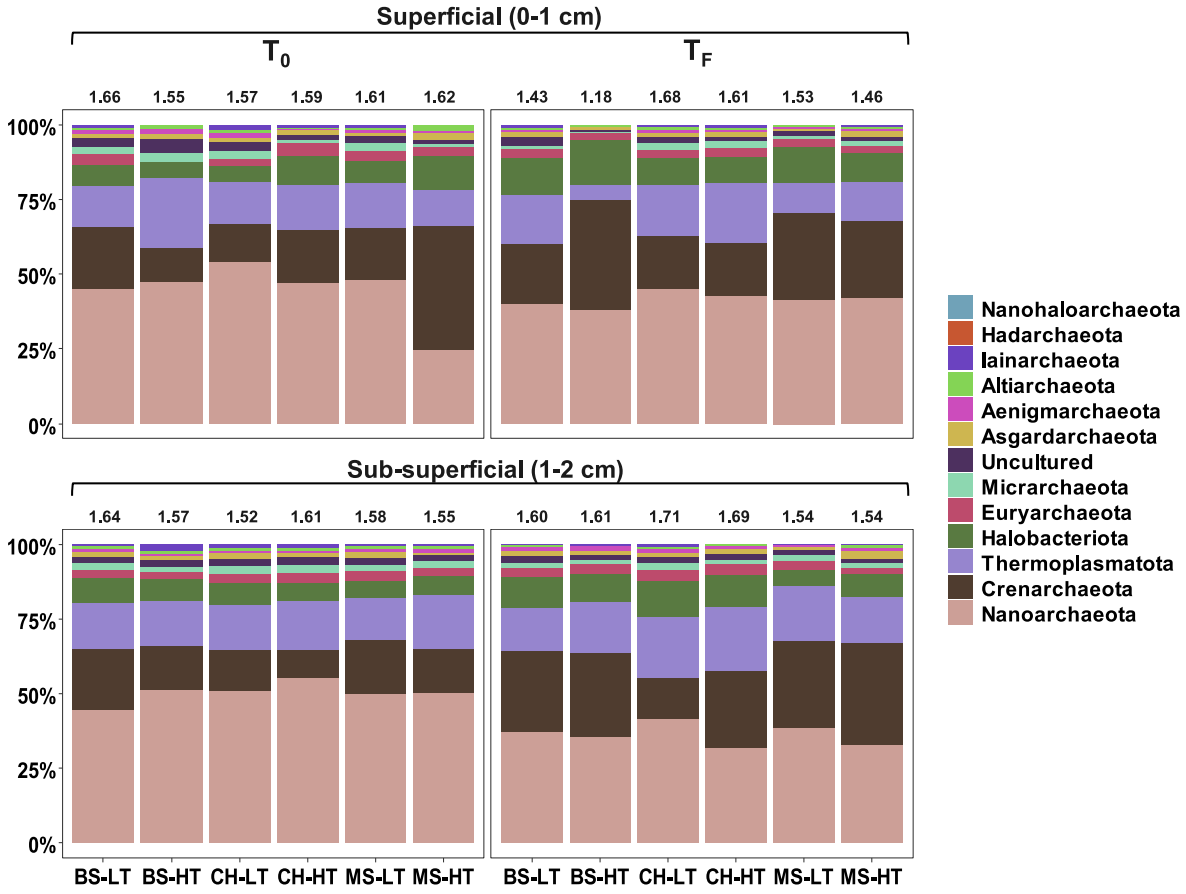

Fig. 7. Barplots of relative abundance of Archaea phyla in the sediment microbial community in the different conditions of each treatment in both layers of sediments (superficial: 0–1 cm, sub-superficial: 1–2 cm) and before planting (T_0) and at the end of the experiment (T_F). Bare sediment (BS), *Chara hispida* (CH) and *Myriophyllum spicatum* (MS); LT: lower temperature; HT: higher temperature. Numbers above each condition column indicate the average of Shannon index values (bits) of the three replicates of each condition.

SCGC_AAA286-E23 with the *Myriophyllum*-treatment. In the bottom sediment, both Archaea phyla and families (Fig. 9G and H) were not significantly separated by the different treatments.

Among methanogenic Archaea, the family Methanosaetaceae was the only one to show statistically significant differences in the final time between conditions, and particularly in the deeper sediment (F_{ANOVA} = 4.0, p = 0.034), the representation of this family being greater in *Chara*-LT compared to the rest of conditions.

Overall, the temperature treatment did not produce significant differences in the microbial structure of the sediment.

3.7. Main variables influencing gas production

Regression analyses separated by plant treatments between dissolved gas concentrations and fluxes showed few significant relationships. The concentration of CH_4 in water was related to TN only in the Bare-sediment treatment (R^2 = −0.66; p = 0.049) and the flux of CH_4 only with DOC concentration in the *Myriophyllum* treatment (R^2 = 0.73; p = 0.031). The CO_2 concentration was not statistically related to any of the physical and chemical variables analyzed, and the flux of CO_2 was positively related to DOC in the *Myriophyllum* treatment (R^2 = 0.77; p = 0.020) and with TP in the *Chara* treatment (R^2 = 0.70; p = 0.038). Regarding the sediment microbial composition, and in terms of families (Table 1), the dissolved CH_4 concentration in water was significantly and positively related to the archaeal families Bathyarchaeia and SCGC_AAA011 in the *Myriophyllum* and *Chara* treatments, respectively, and negatively with a family of the order Micrarchaeales in the *Myriophyllum* treatment. This concentration was positively related to a family of the order Woesearchaeales in the *Chara* treatment, but negatively in the case of the *Myriophyllum* treatment. The flux of CH_4 was positively related to SCGC_AAA286 (also order Woesearchaeales) in the *Myriophyllum* treatment.

4. Discussion

4.1. GHG emissions

As hypothesized (hypothesis 1), and as also found in other studies (Aben et al., 2022; Gremmen et al., 2023), the presence of macrophytes, both the vascular plant and the charophyte, considerably inverted diurnal diffusive CO_2 emissions due to their photosynthetic activity in comparison to bare-sediment situations. When vegetation was present, the system acted as a CO_2 sink while as a source when macrophytes were absent, *M. spicatum* being the species with the largest negative CO_2 fluxes. Despite the similar final biomass reached in each condition (not considering the external carbonate incrustations deposited by *C. hispida*, which is typical for many species of charophytes; Rodrigo et al., 2015), the higher photosynthetic activity of *M. spicatum* is reflected by a higher water pH, higher dissolved oxygen concentrations, the lowest nitrate concentrations, lower DIC and higher DOC concentrations (the latter released by plants, Demarty and Prairie, 2009) measured during the experiment in said treatment. Demarty and Prairie (2009) found no strong link between DOC release rates and concurrent temperature, as observed in this study. Moreover, and according to Simčič and Germ (2010), the respiratory activity of *M. spicatum* was independent of the incubation temperature (three degrees of difference, the same difference

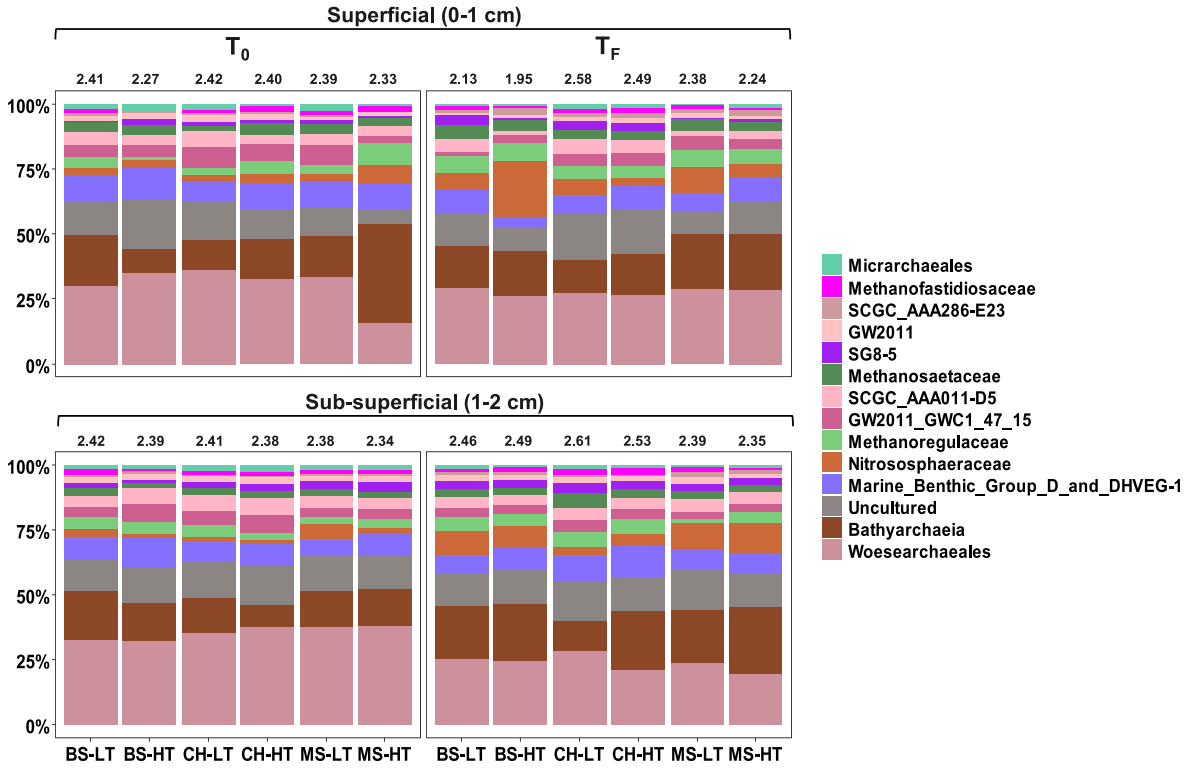

Fig. 8. Barplots of relative abundance of Archaea families in the sediment microbial community in the different conditions of each treatment in both layers of sediments (superficial: 0–1 cm, sub-superficial: 1–2 cm) and before planting (T_0) and at the end of the experiment (T_F). Bare sediment (BS), *Chara hispida* (CH) and *Myriophyllum spicatum* (MS); LT: lower temperature; HT: higher temperature. Numbers above each condition column indicate the average of Shannon index values (bits) of the three replicates of each condition.

as the one used in our experiment), indicating its wide physiological tolerance. The same authors found a lower respiratory potential at higher temperatures in *Chara aspera* and attributed this to an optimized use of energy in this species. All these circumstances would explain why we found little evidence for an important effect of the experimental warming treatment on the diffusive CO_2 flux in the situation with vegetation, converse to what we hypothesized (hypothesis 2). Aben et al. (2022) did not find either a clear positive effect of warmer temperature on this flux in their mesocosms with submerged plant- and algae-dominated systems. In our experiment, although phytoplankton developed in the water of the microcosms (and more at the higher temperature), its influence on the CO_2 emission and dissolved CO_2 concentration was minor because of the low biomass achieved, probably due to the allelopathic activity of both macrophytes (Rojo et al., 2013) on the microalgae, and the lack of phosphorus in the water in the Bare-sediment treatment.

CH_4 diffusion rates ranged from 0 to 0.29 (0.03 on average) mgCH_4/m^2 h which are much lower than the average of around 1.29 mgCH_4/m^2 h found in inland waters (Zheng et al., 2022), but more similar to the annual means from the mesocosm studies of Aben et al. (2022) which obtained 0.19, 0.12 mg CH_4/m^2 h under dominance of submerged plants and algae, respectively. Differential effects of warming on diffusive CH_4 emissions have been reported in the literature, varying from positive effects to the absence of effects (see Aben et al., 2022). Even though both CH_4 production by methanogenic Archaea, mainly in sediments, and microbial oxidation of CH_4, mainly in the sediment-water interface and water column, tend to be temperature dependent (Fuchs et al., 2016), in our case, the temperature increase did not significantly affect CH_4 emissions nor dissolved CH_4 concentrations (converse to hypothesis 2). This might be explained by the lack of apparent warming-induced shifts in the sediment microbial community (see below). Although dissolved CH_4 concentrations were higher in plant treatments, no significant differences were detected in CH_4 diffusive fluxes caused by the presence or absence of plants. This could be because plant development represents a physical barrier for the CH_4 to escape into the atmosphere, as happen with floating plants (Kosten et al., 2016; Schneider et al., 2024), but in this case due to the developed canopy formed by the fine dissected leaves of *M. spicatum* or the thin and numerous branchlets of *C. hispida*), or because plants provide a substrate for methanotrophic bacteria in the water to consume CH_4 before it reaches the water-air interphase (Sorrell et al., 2002; Esposito et al., 2023).

Only in the *Myriophyllum*-treatment were both the CH_4 flux and the dissolved concentration much higher (8-fold and 3-fold, respectively) at the beginning of the incubation time. Other authors, such as Wang et al. (2023) and Grasset et al. (2019), also found higher methanogenic rates at the initial time of their experiments, or observations after adding organic matter, and a decrease afterwards. These findings may be related to the preferential degradation of unstable components of organic matter in the sediments during the first cultivation period, followed by a slower rate of degradation, a process known as the "priming effect" (Bianchi, 2011). The planting of *Myriophyllum* individuals in the bare-sediment, and the start of root development, might have supplied the sediment with organic matter more likely to be used by methanogens.

4.2. The type of macrophyte modifies the microprofile of oxygen in the sediment

Oxygen penetration in sediments is generally limited, typically ranging from tens of microns to a few millimeters (<1 mm in Chesapeake Bay sediments, Kemp et al., 1990; 1–5 mm in sediments influenced by burrows and roots, Meysman et al., 2010; up to 8 mm in incubated sediments, Louati et al., 2013). In this study, we observed oxygen penetration depths of 10 mm in the *Myriophyllum* treatment, 6 mm in the bare-sediment condition, and only 3 mm in the *Chara* treatment. The oxygen extinction rate in the vertical profile was notably

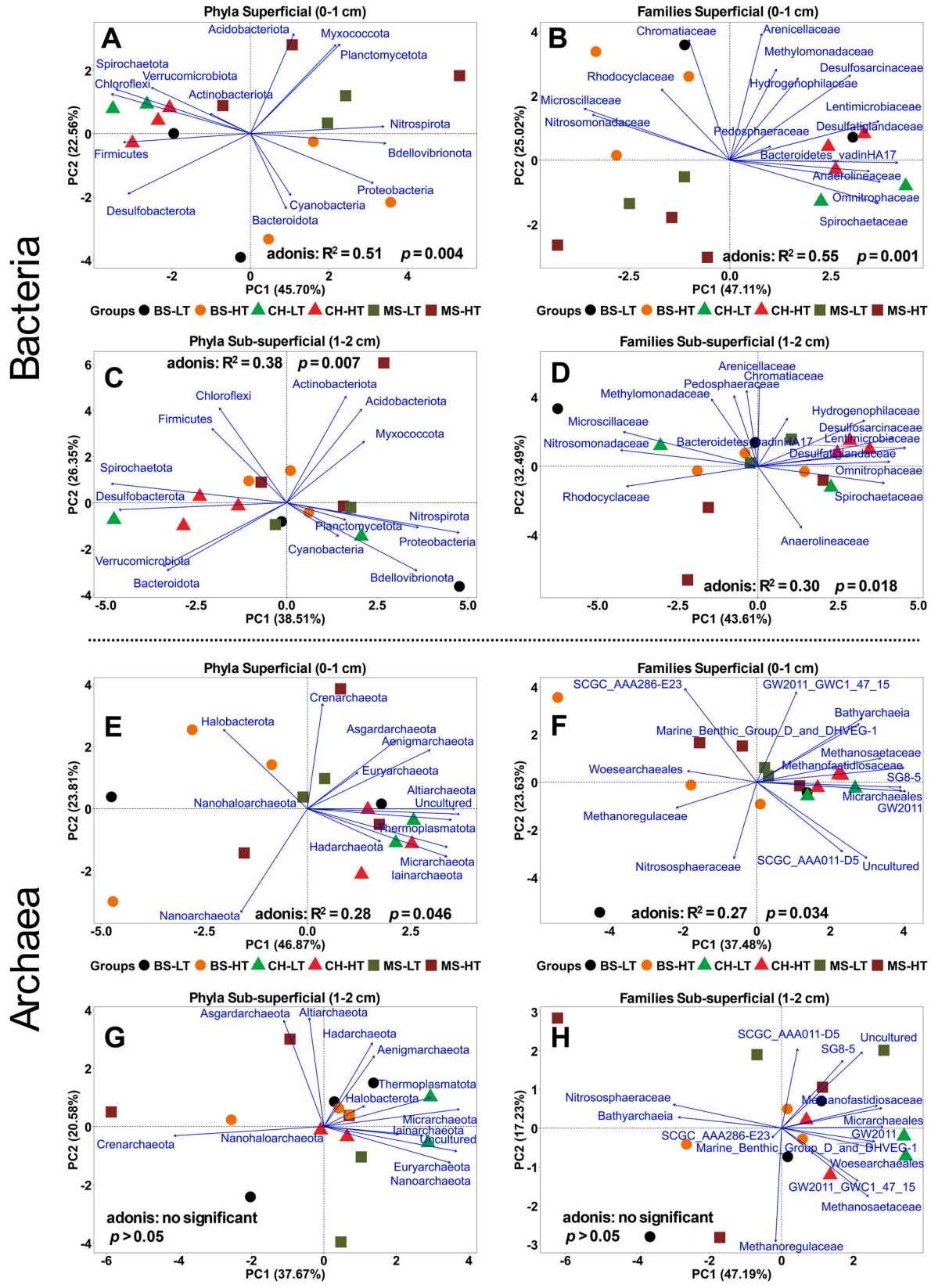

Fig. 9. Principal Component Analysis of the microbial community structure in the different conditions at the end of the experiment, considering bacterial phyla (**A, C**) and families (**B, D**) and Archaea phyla (**E, G**) and families (**F, H**), separated by sediment layer (superficial and sub-superficial). Results of ANOVA analyses (adonis, R^2 and p-value) are also indicated.

Table 1
Significant results of regression analyses between the dissolved concentration of CH_4 in the water column and the CH_4 diffusive flux with the families of sediment bacteria and archaea in the different plant treatments. R^2 and p-value are provided.

	Microorg.	Family	Plant treatment	R^2	p-value
Dissolved CH_4	Arch.	Bathyarchaeia	*Myriophyllum*	0.66	0.048
	Arch.	a family of Micrarchaeales	*Myriophyllum*	−0.74	0.028
	Arch.	a family of Woesearchaeales	*Myriophyllum*	−0.75	0.026
	Arch.	a family of Woesearchaeales	*Chara*	0.61	0.070
	Arch.	SCGC_AAA011	*Chara*	0.82	0.013
	Bacter.	Desulfatiglandaceae	*Chara*	−0.73	0.030
	Bacter.	Desulfosarcinaceae	*Chara*	−0.67	0.045
	Bacter.	Hydrogenophilaceae	*Chara*	−0.96	0.000
	Bacter.	Pedosphaeraceae	*Chara*	−0.75	0.025
	Bacter.	Microscillaceae	Bare sediment	−0.78	0.019
Flux CH_4	Arch.	SCGC_AAA286	*Myriophyllum*	0.73	0.031

faster in the presence of charophytes than in the bare-sediment condition, suggesting that the organic matter accumulated from vegetation likely enhanced microbial oxygen consumption. In contrast, the probable Radial Oxygen Loss (ROL) from *Myriophyllum spicatum* slowed down oxygen depletion, making its profile more similar to the Bare-sediment treatment.

ROL values in wetland macrophytes vary widely, ranging from 0.1 to 2.2 g O_2/m^2·d depending on the species (Lai et al., 2012). While several species within the *Myriophyllum* genus are known to exhibit ROL (Laskov et al., 2006; Herrmann et al., 2009; Kofoed et al., 2012; Sun et al., 2019), data specific to *M. spicatum* are scarce. Laskov et al. (2006) measured a ROL rate of 0.029 mg O_2/h per plant in sandy sediments. Other related species also exhibit low ROL values, such as *M. aquaticum* (0.019 mg O_2/h per plant; Sun et al., 2019), *M. alterniflorum* (minor oxygen release; Herrmann et al., 2009), and *M. verticillatum* (oxygen release localized at root tips; Kofoed et al., 2012). Given our experimental plant density of 344 plants/m^2 and an estimated ROL of 0.024 mg O_2/h per plant, the total oxygen flux from *M. spicatum* roots can be extrapolated to approximately 0.2 g O_2/m^2·d (Sun et al., 2019), a value consistent with previous reports.

While the absolute magnitude of ROL in *M. spicatum* remains relatively low, it was sufficient to maintain a more oxygenated sediment surface compared to the *Chara hispida* treatment, where oxygen was completely depleted at a depth of 3 mm. Unfortunately, the ROL capacity of charophyte rhizoids remains largely unquantified. Our results suggest that, if present, this capacity is negligible to maintain the first centimeter of sediment oxygenated. Thus, the structural differences between vascular macrophytes (*M. spicatum*) and charophytes (*C. hispida*) may not significantly affect functions such as anchorage or nutrient acquisition (Vermeer et al., 2003; Yu et al., 2016), but they do have a substantial impact on sediment oxygenation.

Interestingly, we observed temperature-dependent variations in sediment oxygen microprofiles in the *Myriophyllum* treatment, with higher oxygen concentrations at elevated temperatures. This phenomenon could be linked to an increase in ROL activity under higher temperatures, as previously described in response to water column oxygen availability, sediment redox potential, and microbial oxygen demand (Laskov et al., 2006). However, in our experiment, dissolved oxygen in the water column was generally higher at lower temperatures, particularly toward the end of the study, suggesting a complex interplay between plant physiology and environmental factors.

Another possible mechanism influencing oxygen release is the adjustment of root porosity, a trait observed in *M. spicatum* (Lemoine et al., 2012). Species from eutrophic habitats, which experience frequent anaerobic sediment conditions, have been shown to exhibit higher root porosity and greater ROL compared to species adapted to oligotrophic environments (Lemoine et al., 2012). This could partially explain the enhanced oxygen diffusion in the sediment under the *M. spicatum* treatment compared to the charophyte treatment.

We hypothesized that higher ROL in vascular macrophytes would reduce GHG emissions, particularly methane (CH_4), by promoting aerobic microbial activity. Our results partially support this hypothesis. While dissolved methane concentrations were not consistently lower in the *Myriophyllum* treatment, during the intermediate period of the experiment (from day 10 onward), methane concentrations were clearly lower than in the *Chara* treatment, where more anaerobic conditions prevailed at the sediment surface. However, the observed differences in diffusive CH_4 fluxes between plant treatments were relatively small. This could be due to similar oxygen conditions in the water column across treatments, reducing the potential for differential methane oxidation. In vascular macrophytes such as *M. spicatum*, ROL can create microaerophilic niches within the sediment that support methanotrophic bacteria, which utilize CH_4 as an energy source at oxic-anoxic interfaces (Segers, 1998; Laanbroek, 2010). In contrast, the lack of a true root system in charophytes likely results in more homogeneously anoxic sediment conditions, favoring methanogenesis over methane oxidation.

4.3. Plant effects on the sediment microbial community

The sediment microbial community was different at the microhabitat scale, as the PCA analyses of phyla and families, both bacterial and archaeal, revealed two distinct groups when comparing the 0–1 against the 1–2 cm sediment layer, indicating environmental heterogeneity, mainly caused by the different O_2 concentrations, with the phyla of aerobic bacteria such as Cyanobacteria, Bdellovibrionota, Myxococcota or Proteobacteria (which includes a substantial part of aerobic bacteria) associated with the surficial sediment, and phyla of strict anaerobic bacteria such as Desulfobacterota in the deeper sediment. The warming treatment was not as relevant as the plant treatment, which caused changes in the sediment microbial community structure. However, the highest number of sequences were found in the higher temperature conditions of the plant treatments, suggesting some kind of influence of the temperature on the sediment microorganisms.

In the literature, the effects of aquatic plants on the sediment microbial community are ambiguous. For example, and regarding the plant species closer to those studied here, Karjalainen et al. (2001) described how *Myriophyllum alterniflorum* neither enhanced the bacterial activity nor the microbial biomass in the ambient sediment of a mesotrophic lake in southern Finland under laboratory conditions. However, Germ and Simčič (2011) found a clearer relationship with sediment microbial activity in *M. spicatum* (and other vascular plants such as *Ranunculus circinatus*), but they did not find any permanent biochemical interaction with the sediment for the charophytes *Chara delicatula* and *C. aspera* in an oligotrophic lake. Conversely, our results indicate that *Chara hispida* shapes its rhizobiome, particularly in the more surficial layer of the sediment (0–1 cm), where anoxic conditions are already established, as does *M. spicatum*. Both macrophytes modify this community from the bulk sediment microbial community at the start of the experiment. In the superficial sediment, both bacterial and archaeal communities changed,

and the magnitude of change was similar for both types of microorganisms, as indicated by the beta-diversity index values. However, in the sub-superficial sediment, the archaeal community experienced a slightly greater change with time. The bulk soil can be more rapidly depleted in carbon and other nutrients by heterotrophic microbes, while, in contrast, the rhizosphere created by the presence of these macrophytes serves as a carbon-rich niche (with low-molecular-weight compounds such as organic acids, sugars, amino acids, and other secondary metabolites from the root exudates; Wang et al., 2024) for the establishment of particular microbial communities. However, the aerobic-microaerobic conditions (4–0.2 mgO_2/L) of the superficial sediment caused by the *M. spicatum* ROL can create different functional niches for microorganisms in comparison to the conditions provided by *Chara*. The sediment in the *Chara* treatment contained the highest number of sequences and also the highest diversity of bacterial and archaeal phyla and families in the superficial sediment. High microbial diversity can enhance sediment ecological functions (Li et al., 2022).

Since this is an experiment with the same sediment for all treatments, no exclusive microbial taxa were found. The 16S rRNA gene analyses showed that Proteobacteria (particularly gamma-proteobacteria) was the dominant bacterial phylum in the sediment in our experiment, as usually happens in root environments (Pang et al., 2016). The sediment microbial community mainly consisted of organic carbon degraders (representatives of phyla Proteobacteria, Bacteroidota, Verrucomicrobiota and Chloroflexi -family Anaerolineaceae-), bacteria of the reducing branches (representatives of Desulfobacterota -family Desulfosarcinaceae and Desulfatiglandaceae-) and oxydizing branches (family Hydrogenophilaceae) of the sulphur biogeochemical cycle and the nitrifying bacteria (family Nitrosomonadaceae), methylotrophs (family Methylomonadaceae), photosynthetic microorganisms (representatives of purple sulphur bacteria Chromatiaceae and cyanobacteria), etc. Among bacteria, the phylum Spirochaeta was related to the *Chara*--treatment. Morrison et al. (2017) also found Spirochaeta enriched on *Chara* microcosms in an experiment analyzing the microbial communities which mediate detritus turnover of different algae under anaerobic conditions. The phylum Desulfobacterota was also related to the *Chara*-treatment, as expected due to the anoxic conditions of the sediment.

In the case of Archaea, and compared to bacteria, their representation was very low, in line with other wetlands studies (Puche et al., 2021; Santofimia et al., 2024), but a relatively high representation of phyla was found (12 + 1 –uncultured- out of 21 cited in GTDB (Genome Taxonomy Database, 2025)). The dominant archaeal phyla were Nanoarchaeota, Crenarchaeota and Thermoplasmatota. Moreover, there was a moderate representation of archaeal sequences of uncultured species whose roles cannot be determined. Some authors (Liu et al., 2024) have interpreted the changes in the archaeal community structure as a result of differences in dissolved oxygen, due to the presence of key enzymes with oxygen metabolism in Crenarchaeota that catalyze the reduction of oxygen to water (Vetriani, 2001). In fact, in our experiment, Crenarchaeota is more represented in the *Myriophyllum* treatment, where more O_2 is found in the sediment. We detected microorganisms that can perform a mixture of methanogenic pathways, including the three types: hydrogenotrophic (Methanoregulaceae, more related to the bare-sediment treatment), acetoclastic (Methanosaetaceae) and methylotrophic (Methanofastidiosaceae), both more related to the *Chara*--treatment. This is consistent with the treatments: the methanogens in the sediment with no plants would preferentially use inorganic substances, and the charophyte treatment would provide organic compounds and more anaerobic conditions facilitating the development of acetoclastic and methylotrophic methanogens. Regarding oxidation of methane, the aerobic pathway was represented in our data mainly by the family Methylomonadaceae, which was the fourth family in representation within gamma-proteobacteria, but no statistical differences were found among plant treatments. Besides, nowadays it is known that the anaerobic oxidation of methane involves different electron acceptors, including sulfate, nitrate/nitrite, humic substances, and diverse metal oxides (Zhao et al., 2024), increasing the complexity of the metabolic pathways and complicating the interpretation of the results.

We did not find very many relationships between the flux of gases or the dissolved gas concentrations in the water column with particular microorganisms, but there were some. The concentration of CO_2 and its emission is actively ruled by the photosynthetic activity of the plants, therefore the possible relationships with the bacterial and archaeal community in the sediment might be masked by this important metabolic activity of the vegetation. In the case of the *Myriophyllum* treatment, the dissolved CH_4 was positively related to Bathyarchaeia. Lyu et al. (2018) suggested that the members of this taxon could be methanogens. It is remarkable that the same family of Woesearchaeales, although it probably is not methanogenic, was positively related to dissolved CH_4 in the case of *Chara* and negatively in the case of *Myriophyllum*. Regarding bacteria, the *Chara* treatment was the one with the highest number of statistical relationships with several bacterial families. Wang et al. (2023) found that the activity of methanogenic archaea can be stimulated by algal-organic matter, whereas macrophytic-organic matter mainly increased methanogenic abundance. Since we have not measured activity only relative abundance, finding sound relationships is much more difficult. Further studies on specific functional genes and microorganisms' activities will shed light on these issues.

5. Final remarks and conclusions

Our findings demonstrate the relevance of macrophyte species in determining GHG emissions. This study supports previous results which demonstrated that submerged macrophyte-dominated systems show net CO_2 uptake, while bare-sediment systems (dominated by microalgae) are net emitters of CO_2 and this has great implications for water management because it can determine whether an aquatic ecosystem turns into a carbon source or sink. We are aware that our results have to be extrapolated with caution to more complex natural systems. However, we have observed how, even in the short term, the microbial consortium of the sediments in the different plant treatments was distinct, indicating that the type of plant could recruit specific assemblies. Thus, we have proved that both types of macrophytes have been able to significantly alter the sediment microbial structure. Further studies on functional genes concerning methanogenesis and other processes related to the carbon cycle will elucidate more precisely the influence of these macrophytes on the microbial structure. We have seen how the presence or absence of macrophytes is more important than warming (in our case with a temperature difference of 3 °C) regarding emissions of GHG. Therefore, to substantially mitigate GHG emissions, the management strategies, when restoring or creating new aquatic ecosystems, should favor submerged plant dominance, and particularly the species here assayed (*Myriophyllum spicatum* for more eutrophic systems and *Chara hispida* for more oligotrophic water bodies). Both are characterized to be perennial species, consequently, they can provide their services all year round. Moreover, the particular biological traits such as ROL activity and root porosity, exhibited by *M. spicatum* in our study, are of particular importance in generating special conditions for the development of a particular sediment microbiome. Thus, root functional diversity of submerged vegetation can exert major effects on carbon and nitrogen cycles, and, at the same time, this functional diversity might affect other important ecosystem services such as pollutants uptake in restored aquatic systems.

CRediT authorship contribution statement

María A. Rodrigo: Writing – review & editing, Writing – original draft, Supervision, Project administration, Funding acquisition, Conceptualization. **Eric Puche:** Writing – review & editing, Writing – original draft, Visualization, Methodology, Investigation, Formal analysis, Data curation. **Manuel Muñoz-Colmenares:** Writing – review &

editing, Writing – original draft, Visualization, Methodology, Investigation, Formal analysis, Data curation. **Salvador Sánchez-Carrillo:** Writing – review & editing, Project administration, Methodology, Conceptualization.

Declaration of competing interest

The authors declare that they have no known competing financial interests or personal relationships that could have appeared to influence the work reported in this paper.

Acknowledgements

This study has been funded by projects PID2020-116147 GB-C22 and PID2020-116147 GB-C21 from the Spanish *Ministerio de Ciencia e Innovación*. EP is the holder of a postdoctoral grant (Margarita Salas INV21-03-26) co-founded by Universitat de València and the Spanish *Ministerio de Universidades* with European Union funds (NextGenerationUE). We thank Jose Luis Ayala and Judit Osorio for their guidance with the gas measurements and for the chemical analyses of water samples. Sara García, a master student, helped during the experiment. Daniel Sheerin, a native English teacher and editor, improved the language in the manuscript.

Appendix A. Supplementary data

Supplementary data to this article can be found online at https://doi.org/10.1016/j.jenvman.2025.125654.

Data availability

Raw data are available at: https://roderic.uv.es/items/e30ff10b-5e0d-42c7-a7aa-4f9cc3aa55e1.

References

Aben, R.C.H., Velthuis, M., Kazanjian, G., Frenken, T., Peeters, E.T.H.M., Van de Waal, D. B., Hilt, S., de Senerpont Domis, L.N., Lamers, L.P.M., Kosten, S., 2022. Temperature response of aquatic greenhouse gas emissions differs between dominant plant types. Water Res. 226, 119251. https://doi.org/10.1016/j.watres.2022.119251.

Armstrong, W., 1964. Oxygen diffusion from the roots of some British bog plants. Nature 204, 801–802. https://doi.org/10.1038/204801b0.

Attermeyer, K., Flury, S., Jayakumar, R., Fiener, P., Steger, K., Arya, V., Wilken, F., van Geldern, R., Premke, K., 2016. Invasive floating macrophytes reduce greenhouse gas emissions from a small tropical lake. Sci. Rep. 6, 20424. https://doi.org/10.1038/srep20424.

Azua-Bustos, A., Fairén, A.G., González-Silva, C., Ascaso, C., Carrizo, D., Fernández-Martínez, M., Fernández-Sampedro, M., García-Descalzo, L., García-Villadangos, M., Martín-Redondo, M., Sánchez-García, L., Wierzchos, J., Parro, V., 2018. Unprecedented rains decimate surface microbial communities in the hyperacid core of the Atacama Desert. Sci. Rep. 8, 16706. https://doi.org/10.1038/s41598-018-35051-w.

Benelli, S., Ribaudo, C., Bertrin, V., Bartoli, M., Fano, E.A., 2020. Effects of macrophytes on potential nitrification and denitrification in oligotrophic lake sediments. Aquat. Bot. 167, 103287. https://doi.org/10.1016/j.aquabot.2020.103287.

Bhullar, G.S., Edwards, P.J., Olde, Venterink H., 2013. Variation in the plant-mediated methane transport and its importance for methane emission from intact wetland peat mesocosms. J. Plant Ecol. 6, 298–304. https://doi.org/10.1093/jpe/rts045.

Bhushan, A., Goyal, V.C., Srivastav, A.L., 2024. Greenhouse gas emissions from inland water bodies and their rejuvenation: a review. J. Water Clim. Change 15 (11), 5626–5644. https://doi.org/10.2166/wcc.2024.561.

Bianchi, T.S., 2011. The role of terrestrially derived organic carbon in the coastal ocean: a changing paradigm and the priming effect. Proc. Natl. Acad. Sci. USA. 108, 19473–19481. https://doi.org/10.1073/pnas.1017982108.

Blindow, I., Romanov, R., Schubert, H., Stewart, N., van de Weyer, K., 2024. Chapter 37: Chara hispida. In: Schubert, H., et al. (Eds.), Charophytes of Europe. Springer Nature, Switzerland AG, pp. 527–541. https://doi.org/10.1007/978-3-031-31898-6_37.

Bridgham, S.D., Cadillo-Quiroz, H., Keller, J.K., Zhuang, Q., 2013. Methane emissions from wetlands: biogeochemical, microbial, and modeling perspectives from local to global scales. Glob. Change Biol. 19 (5), 1325–1346. https://doi.org/10.1111/gcb.12131.

Callahan, B.J., McMurdie, P.J., Rosen, M.J., Han, A.W., Johnson, A.J.A., Holmes, S.P., 2016. DADA2: high-resolution sample inference from Illumina amplicon data. Nat. Methods 13, 581e3. https://doi.org/10.1038/nmeth.3869.

Caporaso, J.G., Kuczynski, J., Stombaugh, J., Bittinger, K., Bushman, F.D., Costello, E.K., Fierer, N., González-Peña, A., Goodrich, J.K., Gordon, J.I., Huttley, G.A., Kelley, S.T., Knights, D., Koenig, J.E., Ley, R.E., Lozupone, C.A., McDonald, D., Muegge, B.D., Pirrung, M., Reeder, J., Sevinsky, J.R., Turnbaugh, P.J., Walters, W.A., Widmann, J., Yatsunenko, T., Zaneveld, J., Knight, R., 2010. QIIME allows analysis of high-throughput community sequencing data. Nat. Methods 7, 335e6. https://doi.org/10.1038/nmeth.f.303.

Caporaso, J.G., Lauber, C.L., Walters, W.A., Berg-Lyons, D., Huntley, J., Fierer, N., Owens, S.M., Betley, J., Fraser, L., Bauer, M., Gormley, N., Gilbert, J.A., Smith, G., Knight, R., 2012. Ultra-high-throughput microbial community analysis on the Illumina HiSeq and MiSeq platforms. ISME J. 6 (8), 1621–1624. https://doi.org/10.1038/ismej.2012.8.

Carpenter, S.R., 1996. Microcosm experiments have limited relevance for community and ecosystem ecology. Ecology 77 (3), 677–680. https://doi.org/10.2307/2265490.

CORDIS, 2015. Global warming impacts on stream ecosystems. EU Research Results. https://cordis.europa.eu/article/id/150728-global-warming-impacts-on-stream-ecosystems.

Council Directive, 1992. On the Conservation of Natural Habitats and of Wild Fauna and Flora (92/43/EEC of 21 May 1992).

Demarty, M., Prairie, Y.T., 2009. In situ dissolved organic carbon (DOC) release by submerged macrophyte-epiphyte communities in southern Quebec lakes. Can. J. Fish. Aquat. Sci. 66, 1522–1531. https://doi.org/10.1139/F09-099.

Esposito, C., Nijman, T.P.A., Veraart, A.J., Audet, J., Levi, E.E., Lauridsen, T.L., Davidson, T.A., 2023. Activity and abundance of methane-oxidizing bacteria on plants in experimental lakes subjected to different nutrient and warming treatments. Aquat. Bot. 185, 103610. https://doi.org/10.1016/j.aquabot.2022.103610.

Fox, G.E., Wisotzkey, J.D., Jurtshuk Jr., P., 1992. How close is close: 16S rRNA sequence identity may not be sufficient to guarantee species identity. Int. J. Syst. Evol. Microbiol. 42, 166–170. https://doi.org/10.1099/00207713-42-1-166.

Fuchs, A., Lyautey, E., Montuelle, B., Casper, P., 2016. Effects of increasing temperatures on methane concentrations and methanogenesis during experimental incubation of sediments from oligotrophic and mesotrophic lakes. J. Geophys. Res. 121 (5), 1394–1406. https://doi.org/10.1002/2016JG003328.

Germ, M., Simčič, T., 2011. Vitality of aquatic plants and microbial activity of sediment in an oligotrophic lake (Lake Bohinj, Slovenia). J. Limnol. 70 (2), 305–312. https://doi.org/10.4081/jlimnol.2011.305.

Gremmen, T., van Dijk, G., Postma, J., Colina, M., Domis, L.N.D., Velthuis, M., van de Haterd, R., Kuipers, F., van Rossum, H., Smolders, A.J.P., 2023. Factors influencing submerged macrophyte presence in fresh and brackish eutrophic waters and their impact on carbon emissions. Aquat. Bot. 187, 103645. https://doi.org/10.1016/j.aquabot.2023.103645.

Goldenfum, J.A., 2010. International hydropower association, international hydropower association, unesco, & greenhouse gas status of freshwater reservoirs project. In: GHG Measurement Guidelines for Freshwater Reservoirs. International Hydropower Association (IHA), London, UK.

Grasset, C., Abril, G., Mendonça, R., Roland, F., Sobek, S., 2019. The transformation of macrophyte-derived organic matter to methane relates to plant water and nutrient contents. Limnol. Oceanogr. 64, 1737–1749. https://doi.org/10.1002/lno.11148.

Genome Taxonomy Database, 2025. https://gtdb.ecogenomic.org/. Accessed 25-February-2025.

Harpenslager, S.F., Thiemer, K., Levertz, C., Misteli, B., Sebola, K.M., Schneider, S.C., Hilt, S., Kohler, J., 2022. Short-term effects of macrophyte removal on emission of CO_2 and CH_4 in shallow lakes. Aquat. Bot. 182, 103555. https://doi.org/10.1016/j.aquabot.2022.103555.

Herrmann, M., Saunders, A.M., Schramm, A., 2009. Effect of lake trophic status and rooted macrophytes on community composition and abundance of ammonia-oxidizing prokaryotes in freshwater sediments. Appl. Environ. Microbiol. 75, 3127–3136. https://doi.org/10.1128/AEM.02806-08.

Hessen, D.O., Andersen, T., Armstrong McKay, D., Kosten, S., Meerhoff, M., Pickard, A., Spears, B.M., 2024. Lake ecosystem tipping points and climate feedbacks. Earth Syst. Dynam. 15, 653–669. https://doi.org/10.5194/esd-15-653-2024.

IPCC, 2023. Climate change 2023: synthesis report. Contribution of working groups I. In: Lee, H., Romero, J. (Eds.), II and III to the Sixth Assessment Report of the Intergovernmental Panel on Climate Change [Core Writing Team. IPCC, Geneva, Switzerland, pp. 35–115. https://doi.org/10.59327/IPCC/AR6-9789291691647.

Karjalainen, H., Stefansdottir, G., Tuominen, L., Kairesalo, T., 2001. Do submersed plants enhance microbial activity in sediment? Aquat. Bot. 1–13. https://doi.org/10.1016/S0304-3770(00)00138-8.

Kemp, W., Sampou, P., Caffrey, J., Mayer, M., Henriksen, K., Boynton, W., 1990. Ammonium recycling versus denitrification in Chesapeake Bay sediments. Limnol. Oceanogr. 35 (7), 1545–1563. https://doi.org/10.4319/lo.1990.35.7.1545.

Kofoed, M.V., Stief, P., Hauzmayer, S., Schramm, A., Herrmann, M., 2012. Higher nitrate-reducer diversity in macrophyte-colonized compared to unvegetated freshwater sediment. Syst. Appl. Microbiol. 35, 465–472. https://doi.org/10.1016/j.syapm.2012.08.005.

Kosten, S., Piñeiro, M., de Goede, E., de Klein, J., Lamers, L.P.M., Ettwig, K., 2016. Fate of methane in aquatic systems dominated by free-floating plants. Water Res. 104, 200–207. https://doi.org/10.1016/j.watres.2016.07.054.

Kraemer, B.M., Chandra, s., Dell, A.I., Dix, M., Kuusisto, E., Livingstone, D.M., Schladow, S.G., Silow, E., Sitoki, L.M., Tamatamah, R., McIntyre, P.B., 2017. Global patterns in lake ecosystem responses to warming based on the temperature dependence of metabolism. Glob. Change Biol. 23 (5), 1881–1890. https://doi.org/10.1111/gcb.13459.

Laanbroek, H.J., 2010. Methane emission from natural wetlands: interplay between emergent macrophytes and soil microbial processes. A mini-review. Ann. Bot. 105, 141–153. https://doi.org/10.1093/aob/mcp201.

Lai, W.-L., Zhang, Y., Chen, Z.-H., 2012. Radial oxygen loss, photosynthesis, and nutrient removal of 35 wetland plants. Ecol. Eng. 39, 24–30. https://doi.org/10.1016/j.ecoleng.2011.11.010.

Laskov, C., Horn, O., Hupfer, M., 2006. Environmental factors regulating the radial oxygen loss from roots of *Myriophyllum spicatum* and *Potamogeton crispus*. Aquat. Bot. 84, 333–340. https://doi.org/10.1016/j.aquabot.2005.12.005.

Lemoine, D.G., Mermillod-Blondin, F., Barrat-Segretain, M.-H., Masse, C., Malet, E., 2012. The ability of aquatic macrophytes to increase root porosity and radial oxygen loss determines their resistance to sediment anoxia. Aquat. Ecol. 46, 191–200. https://doi.org/10.1007/s10452-012-9391-2.

Lenth, R.V., 2016. Least-Squares means: the R package lsmeans. J. Stat Softw. 69 (1), 1–33. https://doi.org/10.18637/jss.v069.i01.

Lenth, R.V., 2023. *emmeans*: estimated marginal means, aka least-squares means. R package version 1.8.8. https://CRAN.R-project.org/package=emmeans.

Li, X., Chu, Q., Tang, N., Ogo, H.A., Xing, W., 2022. Functional trait-based potential invasiveness of exotic submerged macrophytes and their effects on sediment bacterial community. Hydrobiologia 849, 3061–3077. https://doi.org/10.1007/s10750-022-04914-9.

Liu, J., Huang, X., Jiang, X., Qing, C., Li, Y., Xia, P., 2024. Loss of submerged macrophytes in shallow lakes alters bacterial and archaeal community structures, and reduces their co-occurrence networks connectivity and complexity. Front. Microbiol. 15, 1380805. https://doi.org/10.3389/fmicb.2024.1380805.

Longhi, D., Bartoli, M., Viaroli, P., 2008. Decomposition of four macrophytes in wetland sediments: organic matter and nutrient decay and associated benthic processes. Aquat. Bot. 89, 303–310. https://doi.org/10.1016/j.aquabot.2008.03.004.

Louati, H., Said, O.B., Got, P., Soltani, A., Mahmoudi, E., Cravo-Laureau, C., Duran, R., Aissa, P., Pringault, O., 2013. Microbial community responses to bioremediation treatments for the mitigation of low-dose anthracene in marine coastal sediments of Bizerte lagoon (Tunisia). Environ. Sci. Pollut. Res. 20 (1), 300–310. https://doi.org/10.1007/s11356-012-0860-x.

Lyu, Z., Shao, N., Akinyemi, T., Whitman, W.B., 2018. Methanogenesis. Curr. Biol. 28 (13), R727–R732. https://doi.org/10.1016/j.cub.2018.05.021.

Meysman, F.J., Galaktionov, O., Glud, R.N., Middelburg, J.J., 2010. Oxygen penetration around burrows and roots in aquatic sediments. J. Mar. Res. 68 (2), 309–336. https://doi.org/10.1357/002224010793721406.

Morrison, J.M., Murphy, C.L., Baker, K., Zamor, R.M., Nikolai, S.J., Wilder, S., Elshahed, M.S., Youssef, N.H., 2017. Microbial communities mediating algal detritus turnover under anaerobic conditions. PeerJ 5, e2803. https://doi.org/10.7717/peerj.2803.

Pang, S., Zhanga, S., Lv, X., Han, B., Liu, K., Qiu, C., Wang, C., Wang, P., Toland, H., He, Z., 2016. Characterization of bacterial community in biofilm and sediments of wetlands dominated by aquatic macrophytes. Ecol. Eng. 97, 242–250. https://doi.org/10.1016/j.ecoleng.2016.10.011.

Paranaíba, J.R., Kosten, S., 2024. Mitigating inland waters' greenhouse gas emissions: current insights and prospects. Inland Waters 14, 97–110. https://doi.org/10.1080/20442041.2024.2372229.

Petersen, J.E., Kemp, W.M., Bartleson, R., Boynton, W.R., Chen, C.C., Cornwell, J.C., Gardner, R.H., Hinkle, D.C., Houde, E.D., Malone, T.C., Mowitt, W.P., Murray, L., Sanford, L.P., Stevenson, J.C., Sundberg, K.L., Suttles, S.E., 2003. Multiscale experiments in coastal ecology: improving realism and advancing theory. Bioscience 53 (12), 1181–1197. https://doi.org/10.1641/0006-3568(2003)053[1181:MEICEI]2.0.CO;2.

Puche, E., Rojo, C., Segura, M., Rodrigo, M.A., 2021. Macrophyte meadows mediate the response of the sediment microbial community to ultraviolet radiation. Hydrobiologia 848, 4569–4583. https://doi.org/10.1007/s10750-021-04662-2.

Puche, E., Roger, B., Vargas-Sánchez, M., Sánchez-Carrillo, S., Rodrigo, M.A., 2025. Freshwater macrophyte type (macroalgae versus phanerogams) mainly determines detritus-derived greenhouse gases production: a microcosm experiment. J. Environ. Sci. https://doi.org/10.1016/j.jes.2025.01.015.

Pukacz, A., Pełechaty, M., Frankowski, M., 2016. Depth-dependence and monthly variability of charophyte biomass production: consequences for the precipitation of calcium carbonate in a shallow *Chara*-lake. Environ. Sci. Pollut. Res. 23, 22433–22442. https://doi.org/10.1007/s11356-016-7420-8.

R Core Team, 2024. R: A Language and Environment for Statistical Computing. R Foundation for Statistical Computing, Vienna, Austria. https://www.R-project.org/.

Ribaudo, C., Benelli, S., Bolpagni, R., Darul, R., Bartoli, M., 2023. Macrophyte growth forms and hydrological connectivity affect greenhouse gas concentration in small eutrophic wetlands. Aquat. Bot. 188, 103660. https://doi.org/10.1016/j.aquabot.2023.103660.

Rodrigo, M.A., Rojo, C., Segura, M., Alonso-Guillén, J.L., Martín, M., Vera, P., 2015. The role of charophytes in a Mediterranean pond created for restoration purposes. Aquat. Bot. 120, 101–111. https://doi.org/10.1016/j.aquabot.2014.05.004.

Rodrigo, M.A., Segura, M., 2020. Plankton participation in the performance of three constructed wetlands within a Mediterranean natural park. Sci. Total Environ. 721, 137766. https://doi.org/10.1016/j.scitotenv.2020.137766.

Rojo, C., Segura, M., Rodrigo, M.A., 2013. The allelopathic capacity of submerged macrophytes shapes the microalgal assemblages from a recently restored coastal wetland. Ecol. Eng. 58, 149–155. https://doi.org/10.1016/j.ecoleng.2013.06.019.

Santofimia, E., González-Toril, E., de Diego, G., Rincón-Tomás, B., Aguilera, A., 2024. Ecological degradation of a fragile semi-arid wetland and the implications in its microbial community: The case study of Las Tablas de Daimiel National Park (Spain). Sci. Total Environ. 924, 171626. https://doi.org/10.1016/j.scitotenv.2024.171626.

Schneider, S.C., Coetzee, J.A., Fukasawa Galvanese, E., Harpenslager, S.F., Hilt, S., Immerzeel, B., Köhler, J., Misteli, B., Motitsoe, S.N., Padial, A.A., Petruzzella, A., Schechner, A., Thiébaut, G., Thiemer, K., Vermaat, J.E., 2024. Causes of macrophyte mass development and management recommendations. Sci. Total Environ. 931, 172960. https://doi.org/10.1016/j.scitotenv.2024.172960.

Segers, R., 1998. Methane production and methane consumption: a review of processes underlying wetland methane fluxes. Biogeochemistry 41 (1), 23–51. https://doi.org/10.1023/A:1005929032764.

Simčič, T., Germ, M., 2010. Increased temperature due to global warming alters the respiratory potential in aquatic organisms from an oligotrophic lake. Int. Rev. Hydrobiol. 95 (4–5), 370–382. https://doi.org/10.1002/iroh.201011213.

Sorrell, B.K., Downes, M.T., Stanger, C.L., 2002. Methanotrophic bacteria and their activity on submerged aquatic macrophytes. Aquat. Bot. 72 (2), 107–119. https://doi.org/10.1016/S0304-3770(01)00215-7.

Su, H.J., Chen, J., Wu, Y., Chen, J.F., Guo, X.C., Yan, Z.B., Tian, D., Fang, J.Y., Xie, P., 2019. Morphological traits of submerged macrophytes reveal specific positive feedbacks to water clarity in freshwater ecosystems. Sci. Total Environ. 684, 578e586. https://doi.org/10.1016/j.scitotenv.2019.05.267.

Sun, H., Xu, S., Wu, S., Wang, R., Zhuang, G., Bai, Z., Deng, Y., Zhuang, X., 2019. Enhancement of facultative anaerobic denitrifying communities by oxygen release from roots of the macrophyte in constructed wetlands. J. Environ. Manage. 246, 157. https://doi.org/10.1016/j.jenvman.2019.05.136, 1.

Theus, M.E., Ray, N.E., Bansal, S., Holgerson, M.A., 2023. Submersed macrophyte density regulates aquatic greenhouse gas emissions. J. Geophys. Res.-Biogeo. 128 (10), e2023JG007758. https://doi.org/10.1029/2023JG007758.

Van den Berg, M.S., Coopsa, H., Simonsb, J., Pilonc, J., 2002. A comparative study of the use of inorganic carbon resources by *Chara aspera* and *Potamogeton pectinatus*. Aquat. Bot. 72, 219–233. https://doi.org/10.1016/S0304-3770(01)00202-9.

Vargas-Sánchez, M., Alcocer, J., Sánchez-Carrillo, S., Oseguera, L.A., Rivera-Herrera, E. M., Soria-Reinoso, I., Guzmán-Arias, A., García-Oliva, F., Merino-Ibarra, M., 2023. Carbon dioxide concentration and emissions along a trophic gradient in tropical karst lakes. Water 15 (1), 13. https://doi.org/10.3390/w15010013.

Vermeer, C.P., Escher, M., Portielje, R., de Klein, J.J.M., 2003. Nitrogen uptake and translocation by *Chara*. Aquat. Bot. 76 (3), 245–258. https://doi.org/10.1016/S0304-3770(03)00056-1.

Vetriani, C., 2001. Archaea, origin of. In: Levin, S.A. (Ed.), In the Encyclopedia of Biodiversity. Academic Press, New York, pp. 219–230.

Wang, T., Zhumabieke, M., Zhang, N., Liu, C., Zhong, J., Liao, Q., Zhang, L., 2023. Variable promotion of algae and macrophyte organic matter on methanogenesis in anaerobic lake sediment. Environ. Res. 237, 116922. https://doi.org/10.1016/j.envres.2023.116922.

Wang, C., Zhu, J., Wang, H., Zhang, L., Li, Y., Zhang, Y., Wu, Z., Zhou, Q., 2024. Sedimentary organic matter load influences the ecological effects of submerged macrophyte restoration through rhizosphere metabolites and microbial communities. Sci. Total Environ. 951, 175419. https://doi.org/10.1016/j.scitotenv.2024.175419.

Webb, J.R., Leavitt, P.R., Simpson, G.L., Baulch, H.M., Haig, H.A., Hodder, K.R., Finlay, K., 2019. Regulation of carbon dioxide and methane in small agricultural reservoirs: optimizing potential for greenhouse gas uptake. Biogeosciences 16, 4211–4227. https://doi.org/10.5194/bg-16-4211-2019.

Wood, S.N., 2006. Generalized Additive Models: an Introduction with R. Chapman and Hall/CRC.

Wood, S.N., Pya, N., Säfken, B., 2016. Smoothing parameter and model selection for general smooth models. J. Am. Stat. Assoc. 111, 1548–1563. https://doi.org/10.1080/01621459.2016.1180986.

Wood, S.N., 2011. Fast stable restricted maximum likelihood and marginal likelihood estimation of semiparametric generalized linear models. J. R. Stat. Soc. B 73 (1), 3–36. https://doi.org/10.1111/j.1467-9868.2010.00749.x.

Woodward, G., Perkins, D.M., Brown, L.E., 2010. Climate change and freshwater ecosystems: impacts across multiple levels of organization. Philos. Trans. R. Soc. Lond. B Biol. Sci. 365 (1549), 2093–2106. https://doi.org/10.1098/rstb.2010.0055.

Yu, J., Zhen, W., Guan, B., Zhong, P., Jeppesen, E., Liu, Z., 2016. Dominance of *Myriophyllum spicatum* in submerged macrophyte communities associated with grass carp. Knowl. Manag. Aquat. Ecosyst. 417, 24. https://doi.org/10.1051/kmae/2016011.

Zhao, Y., Liu, Y., Cao, S., Hao, Q., Liu, Ch, Li, Y., 2024. Anaerobic oxidation of methane driven by different electron acceptors: a review. Sci. Total Environ. 946, 174287. https://doi.org/10.1016/j.scitotenv.2024.174287.

Zheng, Y., Wu, S., Xiao, S., Yu, K., Fang, X., Xia, L., Wang, J., Liu, S., Freeman, C., Zou, J., 2022. Global methane and nitrous oxide emissions from inland waters and estuaries. Glob. Change Biol. 28 (15), 4713–4725. https://doi.org/10.1111/gcb.16233.